Biogeosciences Discuss., doi:10.5194/bg-2016-146, 2016
Manuscript under review for journal Biogeosciences
Published: 30 May 2016

Biogeosciences Discussions
Open Access
EGU

Provenance of branched GDGTs in the Tagus River drainage basin and its outflow in the Atlantic Ocean over the Holocene

Lisa Warden[a], *Jung-Hyun Kim*[a,b], *Claudia Zell*[a,c], *Geert-Jan Vis*[d], *Henko de Stigter*[e], *Jérôme Bonnin*[f], *and Jaap S. Sinninghe Damsté*[a,g]

[a]*NIOZ Netherlands Institute for Sea Research, Department of Marine Microbiology and Biogeochemistry, and Utrecht University, P.O. Box 59, 1790 AB Den Burg, the Netherlan*

[b]*Department of Marine Science and Convergence Technology, Hanyang University ERICA campus, 55 Hanyangdaehak-ro, Sangnok-gu, Ansan-si, Gyeonggi-do 426-791, South Korea*

[c]*Pierre and Marie Curie University - Paris 6 · METIS - UMR 7619 France*

[d]*TNO, Geological Survey of the Netherlands, P.O. Box 80015, 3508 TA Utrecht, the Netherlands*

[e]*NIOZ Netherlands Institute for Sea Research, Department of Ocean Systems Sciences, and Utrecht University, PO Box 59, 1790 AB Den Burg, the Netherlands*

[f]*UMR-EPOC 5805 CNRS, Université de Bordeaux, Allée Geoffroy St Hilaire, 33615 Pessac, France*

[g]*Utrecht University, Faculty of Geosciences, PO Box 80021, 3508 TA Utrecht, the Netherlands*

Correspondence to: Lisa Warden (lisa.warden@nioz.nl)

Keywords: Tagus River basin, Holocene, temperature reconstructions, branched glycerol dialkyl glycerol tetraethers, paleoclimate

Biogeosciences Discuss., doi:10.5194/bg-2016-146, 2016
Manuscript under review for journal Biogeosciences
Published: 30 May 2016

Abstract

The distributions of branched glycerol dialkyl glycerol tetraethers (brGDGTs), which are transported from the soils where they are predominantly produced to marine sediments via rivers, have been applied in reconstructing mean annual air temperatures (MAT) and pH of soils. However, paleoclimate reconstructions using sedimentary brGDGTs have proven difficult in arid regions including the Iberian Peninsula. Recently, six novel 6-methyl brGDGTs have been described using new analytical methods (in addition to the nine 5-methyl brGDGTs previously used for climate reconstructions), and so new pH and MAT calibrations have been developed that in a set of global soil samples were shown to improve the accuracy of reconstructions, especially in arid regions. Because of this we decided to apply the new method to separate the 5- and 6-methyl isomers along with the novel calibrations to a sample set that runs in a transect from source to sink along the Tagus River and out to the deep ocean off the Portuguese margin and spans the last 6,000 years in order to determine if it improves paleoclimate reconstructions in this area. We found that although pH reconstructions in the soils were improved using the new calibration, MAT reconstructions were not much better even with the separation of the 5- and 6-methyl brGDGTs. This confirmed the conclusion of previous studies that the amount of aquatically produced brGDGTs is overwhelming the soil derived ones in marine sediments and complicating MAT reconstructions in the region. Additionally, the new separation revealed a strong relationship between the new degree of cyclization (DC') of the brGDGTs and MAT not seen before that could be making temperature reconstructions in this and other arid regions difficult.

Biogeosciences Discuss., doi:10.5194/bg-2016-146, 2016
Manuscript under review for journal Biogeosciences
Published: 30 May 2016

1. Introduction

Understanding past climate variability is important for predicting future climate change as well as how ecosystems, organisms and human society could be affected. The validation of climate proxies is imperative for the correct interpretation of climate archives and therefore also for the climate models building on these past climate data. Terrestrial environments play an important role in global climate, however, continental climate reconstructions are hindered by the lack of continental temperature proxies. In the future, changes in terrestrial climate are likely to have a large impact on human society just as they had in the past (e.g. Haug et al., 2003). Availability of trustworthy temperature data from the terrestrial environment will be essential for the development of reliable climate models.

The distribution of branched glycerol dialkyl glycerol tetraethers (brGDGTs, Fig. S1), a group of membrane-spanning lipids that occur in heterotrophic bacteria (Pancost and Sinninghe Damsté, 2003; Weijers et al., 2010) pervasive in peat (Weijers et al., 2006) and worldwide in soils has proven useful as a tool to obtain high resolution, continental temperature reconstructions (Weijers et al., 2007a; Schouten et al., 2008; Bendle et al., 2010). BrGDGTs are biosynthesized by bacteria (Sinninghe Damsté et al., 2011; 2014) living in soils and the distribution of brGDGTs in soils is affected by growth temperature and pH (Weijers et al., 2006). More specifically, the degree of methylation of the brGDGTs (expressed as methylation of branched tetraethers index, MBT) relates to mean annual air temperature (MAT), and to a lesser extent soil pH, whereas the degree of cyclization (DC) of the brGDGTs (also expressed as the cyclization of branched tetraethers index, CBT) correlates solely with soil pH (Weijers et al., 2007a). MBT has recently been amended to become MBT' by eliminating the brGDGTs that rarely occur in soils (Peterse et al., 2012). These observations led to the development of a continental paleoclimate proxy based on the distribution of brGDGTs that has been applied in paleosoils (Peterse et al., 2009; Weijers et

Biogeosciences Discuss., doi:10.5194/bg-2016-146, 2016
Manuscript under review for journal Biogeosciences
Published: 30 May 2016

al., 2007a; 2011). Branched GDGTs that are produced in soils are washed by runoff into streams and rivers where they are transported to and deposited in river sediment and in coastal marine sediment that are under the influence of major river systems. In this way, brGDGTs have been used as recorders of the continental paleoclimate (Weijers et al., 2007b; Bendle et al., 2010; Hren et al., 2010; Keating-Bitonti et al., 2011).

Complications using brGDGTs as a proxy for MAT have arisen in some settings. In marine sediments receiving a low input of soil organic matter (OM), it was found that the distribution of brGDGTs and the reconstructed temperatures were quite different from that observed in regional soils (Peterse et al., 2009). Peterse et al. (2012) found in arid regions temperature is no longer an important control on the distribution of brGDGTs and therefore MAT reconstructions in these areas should be interpreted with care. In the Iberian Peninsula, Menges et al. (2013) found that MBT' was not correlated to MAT but instead correlated with the aridity index (AI), a parameter for water availability in soils, and mean annual precipitation (MAP). In drainage basins with varying soil sources that had different MATs (i.e. mountainous vs. lowland), it was found that the provenance of the soil matter must be considered when interpreting MAT reconstructions (Bendle et al., 2010). In-situ production of brGDGTs can occur within the river systems (Yang et al., 2012; Zell et al., 2013, De Jonge et al., 2014b) and cause brGDGT distributions and MAT reconstructions that differ from those in the soils of the source area. These complications make it vital to investigate how varying environmental conditions, the transport of these terrestrially derived fossilized lipids, and in-situ production affect the implementation of brGDGTs for paleoclimate reconstructions.

Recently a set of six new brGDGT isomers that differ in the position of the methyl groups were identified and described (De Jonge et al., 2013). The relative abundance of these novel, 6-methyl brGDGTs are strongly dependent on pH and so by excluding them from the MBT' index (newly defined as MBT'_{5ME}) the correlation with MAT is improved (De Jonge et

Biogeosciences Discuss., doi:10.5194/bg-2016-146, 2016
Manuscript under review for journal Biogeosciences
Published: 30 May 2016

al., 2014a). The CBT index was also redefined in this study, as CBT', to include all of the pH dependent 6-methyl brGDGTs and consequently yielded a higher correlation with soil pH as a result (De Jonge et al., 2014a). De Jonge et al. (2014a) also developed, based on a dataset of globally distributed soils, a new pH calibration taking into account the new CBT' as well as new MAT calibrations, defined as MAT_{mr} and MAT_{mrs}. In a global soil set they were shown to improve the accuracy of reconstructions, especially in arid regions. These indices and calibrations were applied in a coastal sediment core in the Northern Kara Sea off Siberia in a study emphasizing the importance of examining the provenance of brGDGTs when using these lipids for paleoclimate reconstructions (De Jonge et al., 2015).

A comprehensive study has been previously performed on the present day transport of brGDGTs in the Tagus River basin from source to sink (Zell et al., 2014). The results from this study demonstrated that the distribution of brGDGTs in the riverine suspended particulate matter (SPM) did not reflect that of the soils, implying that due to the aquatic production in river and marine environments the use of brGDGTs for paleoclimate reconstructions in the region would be complicated (Zell et al., 2014; 2015). Here we examine if the assessment of the provenance of brGDGTs in the Tagus River basin can be improved by the application of the analytical methods allowing the separation of the 5- and 6-methyl brGDGTs (De Jonge et al., 2013). In addition, we examine if the provenance of brGDGTs changed over the Holocene and if the distribution of brGDGTs in the past reflected continental sources and thus past temperature and pH of the soils in the drainage basin of the river. To this end we compare the down core brGDGT distributions in Holocene sediments retrieved from four locations along a transect in the Tagus River basin, which includes the river floodplain (Tagus River Floodplain core), the offshore mudbelt (Mudbelt core), and marine sediments from the canyons (Lisbon Canyon Head core and Lower-Sétubal canyon core) (Fig. 1), and compare them to brGDGT distributions of soil and river SPM from the Tagus River watershed. This allows insight into

Biogeosciences Discuss., doi:10.5194/bg-2016-146, 2016
Manuscript under review for journal Biogeosciences
Published: 30 May 2016

125 the potential and limitations of using the novel MAT_{mrs}/CBT' proxies for climate
126 reconstruction in this region and in river systems in general.
127

128 **1. Study Area**

129 The Tagus River drains the central part of the Spanish Plateau with an E-W orientation
130 (Benito et al., 2003). The waters originate at an elevation of about 1600 m altitude in eastern
131 Spain at the Iberian Range and the mouth of the river feeds into the Atlantic Ocean near
132 Lisbon (Vis and Kasse, 2009). At 1,200 km long the Tagus River is the longest river of the
133 Iberian Peninsula and it occupies 82×10^3 km^2 making it the third largest in catchment area
134 (Benito et al., 2003). The Tagus Basin is surrounded by mountains on three sides with the
135 Iberian Range to the east, the Central Range to the north, and the Toledo Mountains to the
136 south. Present-day mean discharge at the Tagus River mouth is 400 m^3 s^{-1} (Vale and Catarino,
137 1996; Vaz et al., 2011) and the largest contribution of draining tributaries comes from the
138 Central Range in the North (Benito et al., 2003). The Tagus River is characterized by extreme
139 seasonal and annual variability, including periods of flooding with 30 times the mean
140 discharge and an annual discharge cycle characterized by two peaks in the winter (December
141 and then again February to March) and a discharge minimum in the summer (August) (Benito
142 et al., 2003). Since the 1940s dams have been built along the expanse of the Tagus River for
143 water supply, hydropower, and flood prevention (Dias et al., 2002), which have likely
144 impacted the transport of brGDGTs in the Tagus River system since their construction.
145 Where the Tagus River debouches into the Atlantic Ocean, the narrow continental shelf
146 and steep continental slope are deeply incised by the Lisbon-Setúbal canyon system. The head
147 of the Lisbon branch of that canyon system is located 13 km offshore from the Tagus River
148 mouth at 120 m water depth. From that point, the canyon descends over a length of 165 km
149 until it opens out onto the Tagus Abyssal Plain at 4860 m (Lastras et al., 2009). Even though

Biogeosciences Discuss., doi:10.5194/bg-2016-146, 2016
Manuscript under review for journal Biogeosciences
Published: 30 May 2016

the shelf is very narrow, sparse amounts of continental organic matter and clastic sediment reach the deep ocean in this region (Jouanneau et al., 1998; de Stigter et al., 2011; Vis et al., in press). This is because the Lisbon-Setúbal canyon is not a very dynamic system and has a weak down-canyon transport of sediments (Jouanneau et al., 1998; Jesus et al., 2010; de Stigter et al., 2011). A part of the continental shelf in this region is covered by mud deposits, which originate predominantly from the Tagus estuary (Jouanneau et al., 1998). According to this same study, the mouth of the much smaller Sado River is located further to the southeast and contributes only a relatively minor sediments volume to the shelf mud deposits.

Generally, the climate of the Tagus River Basin is characterized by seasonal variability and is considered continental Mediterranean (Le Pera and Arribas, 2004). Summers in the Tagus region are hot and dry and the winters are relatively mild and wet (Benito et al., 2003). During the summers, the climate regime in the Tagus Basin is controlled by the Azores high and in the winter by the westerlies (Benito et al., 2003). The MAT in the interior regions of the Tagus River basin varies from the highlands to the lowlands of the inner basin from 7.5 to 12.5°C, respectively and can increase up to 16°C along the Atlantic Coast (Le Pera and Arribas, 2004). The mean annual precipitation in the lowlands of the inner basin is mostly below 500 mm making it an arid region, however, some of the highest altitudes of the mountainous areas have a larger mean annual precipitation ranging from 750-1200 mm (Le Pera and Arribas, 2004).

The Iberian Peninsula is located between two major pressure systems, the Azores High and the Iceland Low, which make up the North Atlantic Oscillation (NAO). This climate phenomenon is caused by the varying pressure gradient in the North Atlantic and greatly influences climate conditions all over Europe (Hurrell, 1995; Hurrell and VanLoon, 1997). Because of the Iberian Peninsula's advantageous position for studying the shifting NAO, the climate in this region has been intensively investigated (Zorita et al., 1992; Rodó et al., 1997;

Biogeosciences Discuss., doi:10.5194/bg-2016-146, 2016
Manuscript under review for journal Biogeosciences
Published: 30 May 2016

175 Trigo et al., 2004). Many of these studies are from an oceanic perspective, obtaining sea
176 surface temperatures from marine sediments using the alkenone unsaturation indices
177 (Abrantes et al., 2005, 2009; Rodrigues et al., 2009), coccolithophore assemblages (Cachao
178 and Moita, 2000; Palumbo et al., 2013), and stable isotopic oxygen composition of
179 foraminifera (Lebreiro et al., 2006 ; Bartels-Jónsdóttir et al., 2006; 2009). The terrestrial
180 climate has been examined using continental paleoarchives such as speleothems (Munoz-
181 Garcia et al., 2007; Martin-Chivelet et al., 2011; Stoll et al., 2013), tree rings (Andreu et al.,
182 2007; Linan et al., 2012), and pollen (Huntley and Prentice, 1988; Lebreiro et al., 2006; Davis
183 et al., 2003; Fletcher et al., 2007; Corella et al., 2013). The integrated continental and marine
184 approach can give complimentary information to past climate in a region and by using the
185 same proxy on the continent, in the ocean, and at the ocean-continent interface we would
186 perhaps obtain a clearer picture of continental climate processes in an area rather than using
187 separate studies or a multi-proxy approach.
188

189 ## 2. Material and Methods

190 **Sample collection**. Soil samples, riverbank sediment samples, and river SPM from the Tagus
191 River basin (Fig. 1b) were collected previously (Zell et al., 2014). These samples were
192 complemented with four long sediment cores collected along a transect running from the
193 Tagus River to the lower continental slope (Fig. 1). The Tagus River Floodplain core
194 (0501.029) was collected in a low-energy backswamp of the present-day floodplain of the river
195 at ~4 km west of the Tagus channel (Table 1). The sediment was collected using an Edelman
196 hand auger for sediment above the groundwater table and a gauge for sediment below the
197 groundwater table (Vis et al., 2008). The sediments were wrapped in the field for laboratory
198 analyses. The other three cores were collected using a piston corer, during campaigns in May
199 2007 and March 2011 with RV *Pelagia* conducted by the NIOZ - Royal Netherlands Institute

Biogeosciences Discuss., doi:10.5194/bg-2016-146, 2016
Manuscript under review for journal Biogeosciences
Published: 30 May 2016

for Sea Research. The coring site for the Mudbelt core (64PE332-30-2) was to the west of the Tagus Estuary mouth, for the Lisbon Canyon Head core (64PE332-44-2) it was to the east of the Tagus Estuary mouth, and for the Lower Setúbal Canyon core (64PE269-39) it was on the crest of the northern levee of the lower Setúbal Canyon (Table 1).

Age models. The accelerated mass spectrometry (AMS) ^{14}C measurements of the three marine sediment cores were carried out at the BETA analytic laboratory (USA) on benthic or planktonic forams, gastropods or shells fragments (Table 2). As for the Tagus River Floodplain core, the radiocarbon dating material was performed for a previous study and consisted of mostly terrestrial botanical macrofossils, but other bulk material was used as well (Vis et al., 2008). In order to establish consistent chronologies for the four sediment cores, all the AMS dates were calibrated into calendar ages using the CALIB 7.0, available at http://radiocarbon.pa.qub.ac.uk/calib (Stuiver et al., 1998). The calibration data and curve selection used for the three marine sediment cores was Marine13 and for the Tagus River Floodplain core IntCal13 was used (Reimer et al., 2013). All radiocarbon dates mentioned have age spans at the 2σ range and are expressed as calibrated ages (cal. BP) (Table 2, Fig. S2).

Bulk isotope data Prior to bulk carbon isotope analysis, sediment was decalcified using a 2 N HCL solution for approximately 18 h. The sediment was rinsed three times using double-distilled water and then freeze dried again. Total organic carbon (TOC) and $\delta^{13}C_{TOC}$ (Table 3) were measured in duplicate using the Flash 2000 series Organic Elemental Analyzer (Thermo Scientific) equipped with a TCD detector. The $\delta^{13}C_{TOC}$ is expressed in relation to the Vienna PeeDee Belemnite (VPDB) standard and the isotope analysis precision was 0.1‰.

Biogeosciences Discuss., doi:10.5194/bg-2016-146, 2016
Manuscript under review for journal Biogeosciences
Published: 30 May 2016

224

225 **Lipid extraction and GDGT analysis.** Between 1-3 g of freeze dried sediment was extracted
226 using the Dionex™ accelerated solvent extraction (ASE) with dilchloromethane
227 (DCM):methanol (9:1, v/v) as the solvent at a temperature of 100°C and a pressure of 1500
228 psi for 5 min with 60 % flush and purge 60 seconds. The extract was then collected and dried
229 using Caliper Turbovap®LV. Next, using DCM, the lipid extract was dried over a column of
230 anhydrous Na_2SO_4 and then blown down under a gentle stream of N_2. In order to quantify
231 GDGTs, 1 µg of an internal standard (C_{46} GDGT; Huguet et al., 2006) was added to the total
232 lipid extract before it was separated over a ccolumn of Al_2O_3 (activated for 2 h at 150°C) into
233 three fractions using hexane:DCM (9:1, v:v) for the apolar fraction, hexane:DCM (1:1, v:v)
234 for the ketone fraction and DCM:MeOH (1:1, v:v) for the polar fraction. The polar fraction,
235 which contained the GDGTs, was dried under a N_2 stream and then re-dissolved in
236 hexane:isopropoanol (99:1, v:v) at a concentration 10 mg ml^{-1}. Finally it was passed through a
237 0.45 µm PTFE filter and analysed with high performance liquid chromatography-atmospheric
238 pressure positive ion chemical ionization–mass spectrometry (HPLC-APCI-MS) with a
239 separation method that allows the separation of 5- and 6-methyl brGDGTs (Hopmans et al.,
240 2015). For the study of Zell et al., (2014) the samples were split into two different fractions
241 before the analysis, the intact polar lipid (IPL) fraction and core lipid (CL) fractions. For the
242 purposes of this study the IPL and CL fractions of the river SPM were analyzed separately on
243 the HPLC-APCI-MS for GDGTs (Hopmans et al., 2015) and then the amount of GDGTs
244 found in the CL and IPL fractions were combined. After analysis some of the GDGT based
245 indices were recalculated for the entire sample set.

246

Biogeosciences Discuss., doi:10.5194/bg-2016-146, 2016
Manuscript under review for journal Biogeosciences
Published: 30 May 2016

247 **Calculation of GDGT-based proxies.** The Roman numerals refer to the GDGTs indicated in
248 Fig. S1. The 5-methyl brGDGTs and 6-methyl brGDGTs are distinguished by an accent on
249 the 6-methyl brGDGTs. The GDGT indicated by IV is crenarchaeol, the isoprenoid GDGT
250 specific to Thaumarchaeota (Sinninghe Damsté et al., 2002).

251 The BIT Index (Hopmans et al., 2003) was calculated using the following formulae that
252 specifically includes the novel 6-methyl brGDGTs according to De Jonge et al. (2015):

253 BIT index = (Ia+IIa+IIIa+IIa'+IIIa')/(Ia+IIa+IIIa+IIa'+IIIa'+IV) (1)

254 The isomer ratio (IR) signifies the quantity of the penta- and hexamethylated 6-Me brGDGTs
255 compared to the total brGDGTs and was calculated according to De Jonge et al., (2015):

256 IR=(IIa'+IIb'+IIc'+IIIa'+IIIb'+IIIc')/(IIa+IIb+IIc+IIIa+IIIb+IIIc+IIa'+IIb'+IIc'+IIIa'+IIIb'+
257 IIIc') (2)

258 The relative abundance of the penta- and hexamethylated 6-methyl brGDGTs are calculated
259 according to (De Jonge et al., 2014b):

260 IR_{II}= IIa'/(IIa+IIa') (3)

261 IR_{III} = IIIa'/(IIIa+IIIa') (4)

262 The MBT'_{5Me} (which excludes the 6-methyl brGDGTs) was used to calculate MAT according
263 to De Jonge et al., (2014a):

264 MBT'_{5Me} = (Ia+Ib+Ic)/(Ia+Ib+Ic+IIa+IIb+IIc+IIIa) (5)

265 MAT = -8.57 +31.45* MBT'_{5Me} (6)

266 The equation to determine DC (Sinninghe Damsté et al., 2009) was reformulated to
267 specifically include the pentamethylated 6-methyl brGDGTs:

Biogeosciences Discuss., doi:10.5194/bg-2016-146, 2016
Manuscript under review for journal Biogeosciences
Published: 30 May 2016

$$DC' = (Ib+IIb+IIb')/(Ia+Ib+IIa+IIb+IIa'+IIb') \quad (7)$$

To calculate pH and MAT the novel MAT_{mr} /CBT' calibration was used (De Jonge et al., 2014a):

$$CBT' = {}^{10}\log[(Ic+IIa'+IIb'+IIc'+IIIa'+IIIb'+IIIc')/(Ia+IIa+IIIa)] \quad (8)$$

$$pH = 7.15 + 1.59 * CBT' \quad (9)$$

$$MAT_{mr} = 7.17 + 17.1 * [Ia] + 25.9 * [Ib] + 34.4 * [Ic] - 28.6 * [IIa] \quad (10)$$

$$MAT_{mrs} = 5.58 + 17.91 * [Ia] – 18.77* [IIa] \quad (11)$$

Statistical analysis. Using R software package for statistical analysis we performed principal component analysis (PCA) based on the correlation matrix. We performed the PCA on the fractional abundances of all 15 of the 5- and 6-methyl brGDGTs for the entire sample set along the transect from the land to the ocean.

3. Results

We report bulk and brGDGT data for four cores covering Holocene sedimentation in the Tagus River Basin and its outflow into the Atlantic. We compare these data with new results acquired through an improved LC method able to distinguish between the 5- and 6-methyl brGDGTs (De Jonge et al., 2013) on the soils, riverbank sediments, and SPM samples previously obtained by Zell et al., (2014).

4.1 Bulk parameters of the sediments

Biogeosciences Discuss., doi:10.5194/bg-2016-146, 2016
Manuscript under review for journal Biogeosciences
Published: 30 May 2016

289 The age-depth models for the marine sediment cores (Fig. S2, Table 1) are based on
290 radiocarbon dating of picked foraminifera, gastropods, and shell fragments. The data show
291 that of the four sediment cores from the transect the Tagus River Floodplain sediments date to
292 6.7 cal. kyrs. BP, the Mudbelt sediments date to 5.8 cal. kyrs. BP, the Lisbon Canyon Head
293 sediments date to 8.7 cal. kyrs. BP, and the Lower Setúbal Canyon penetrated the oldest strata
294 (13.0 cal. kyrs. BP). Reported values for sediments from each location were averaged over the
295 interval 0-6.0 cal. kyrs. BP, so as to avoid a bias in the data since not all of the sediment cores
296 covered more than 6.0 kyrs.

297 The bulk carbon isotope data for the Tagus River SPM, riverbank sediments, and soils
298 has been previously discussed in Zell et al., (2014). The TOC values for the Tagus River
299 Floodplain sediments are relatively high and also highly variable with a range of 1.5-16 wt. %
300 and a mean of 6.5±4.3 wt. % (average ± standard deviation) and the mean $\delta^{13}C_{TOC}$ was -
301 27.0±1.0 ‰ (Fig. 2; Table 3). In the Mudbelt sediments the TOC is less variable than in the
302 Tagus River Floodplain sediments, ranging from 0.6-1.2 wt. % and with an average of
303 0.9±0.2 wt. % (Fig. 2; Table 3). The average $\delta^{13}C_{TOC}$ in the Mudbelt sediments, -24.3±0.2 ‰,
304 is higher than in the Tagus River Floodplain sediments. The average $\delta^{13}C_{TOC}$ of the Lisbon
305 Canyon Head sediments, -23.0±0.6 ‰, is higher than the Mudbelt sediments and the TOC
306 content is similar to that of the Mudbelt sediments, ranging from 0.25-1.5 wt. % with the
307 mean of 0.9±0.3 wt. % (Fig. 2; Table 3). The average $\delta^{13}C_{TOC}$ values in the Lower Setúbal
308 Canyon sediments (-23.4±1.5‰) are similar to those of the Lisbon Canyon Head sediments
309 with a TOC content ranging from 0.51-0.85 wt. % with a mean value of 0.65±0.14 wt. % (Fig.
310 2; Table 3).

311

312 **4.2 Concentrations and distribution of GDGTs**

Biogeosciences Discuss., doi:10.5194/bg-2016-146, 2016
Manuscript under review for journal Biogeosciences
Published: 30 May 2016

313 *Tagus Soils and Riverbank Sediments.* The average concentration of crenarchaeol is
314 higher in the riverbank sediments (~8.7±7.8 µg gOC^{-1}) than in the soils (~1.4±1.1 µg gOC^{-1})
315 (Fig. 3a-b; Table 3). The same trend is true for the brGDGTs with the average concentration
316 being higher in the riverbank sediments (~33.9±24.5 µg gOC^{-1}) than the soils (~6.8±6.5 µg
317 gOC^{-1}) (Fig. 3a-b; Table 3). The values of the BIT index were similar to those previously
318 reported (Zell et al., 2014) for both the soils and riverbank sediments and ranged from 0.3 to
319 1.0 with an average of 0.7±0.2 (Fig. 3c; Table 3). The re-analysis of the brGDGTs in the soils
320 reveals that the relative abundance of the novel 6-methyl brGDGTs is highly variable (ranging
321 from 0.13-0.92) and can be quite high; the average values for the IR are 0.6±0.3 (Fig. 3e;
322 Table 3). IR is even higher but less variable for the riverbank sediments with an average of
323 0.7±0.1 (Fig. 3e; Table 3). In general the penta- and hexamethylated brGDGTs show the same
324 ratio of 5- and 6-methyl isomers (Fig. 4), however, in soils from an altitude of >350 m the 6-
325 methyl brGDGTs are especially dominant (Fig. S4). Values for the new MBT'_{5me} index,
326 which excludes the 6-methyl brGDGTs (cf. De Jonge et al., 2014a), of the soils and riverbank
327 sediments are quite similar with an average of 0.5±0.1 in both cases (Fig. 3f; Table 3). The
328 DC' ratio deviates between the soils and the riverbank sediments (Fig. 3d; Table 3). The DC'
329 for the soils is highly variable but on average low (0.2±0.1); for the riverbank sediments it is
330 higher with an average of 0.4±0.1.

331 *Tagus River SPM.* The SPM was obtained from the Tagus Estuary near the mouth of
332 the Tagus River once a month over the course of a year (excluding the month of August).
333 Data from the Tagus River SPM showed that the summed brGDGT and crenarchaeol
334 concentrations in the river SPM varied throughout the year and were on average 45±23 µg
335 gOC^{-1}, and 9.8±6.8 µg OC^{-1}, (Figs. 3a-b; Table 3), respectively, resulting in only small
336 variations in the BIT index (i.e. 0.8±0.1; Fig. 3c; Table 3). The distribution of brGDGTs (Fig.

Biogeosciences Discuss., doi:10.5194/bg-2016-146, 2016
Manuscript under review for journal Biogeosciences
Published: 30 May 2016

337 5c) was relatively constant throughout the year as is evident from the values for MBT'$_{5me}$
338 (0.5±0.0), DC' (0.3±0.0), and IR (0.6±0.0) for the river SPM (Figs. 3d-f; Table 3).

339 *Tagus River Floodplain sediments.* The average crenarchaeol concentration is fairly
340 low in the Tagus River Floodplain sediments, 2.8±1.7 µg gOC^{-1}, conversely, the average sum
341 of the brGDGTs in the sediments, 70±26 µg gOC^{-1}, is the largest out of the entire transect
342 (Figs. 3a-b; Table 3). The BIT index is fairly high and constant throughout the sediment core
343 with an average value of 0.9±0.0 (Fig. 3c; Table 3). The distribution of brGDGTs (Fig. 5d) is
344 somewhat similar to that of the riverine SPM (Fig. 4c) and shows no major changes over the
345 Holocene. The Tagus River Floodplain sediments has the lowest average values for MBT'$_{5me}$,
346 0.4±0.1, and IR, 0.4±0.0, of all the sediment records in the transect (Figs. 3e-f). The mean
347 DC' throughout the sediments in this sample set is 0.4±0.1 (Fig. 3d; Table 3).

348 *Mudbelt sediments.* The average concentration of the brGDGTs, 25±14 µg gOC^{-1}, is
349 lower than in the Tagus River Floodplain sediments, however, the concentration of
350 crenarchaeol, 170±50 µg gOC^{-1}, is higher in the Mudbelt sediments (Figs. 3a-b; Table 3). This
351 results in a lower mean value of the BIT index (i.e. 0.09±0.03; Fig. 3c; Table 3). The brGDGT
352 distribution is relatively constant over the Holocene and is fairly similar to that of the Tagus
353 River floodplain sediments with slightly higher fractional abundances of Ia and IIIa' (cf. Figs.
354 5d-e; Table 3). The average value of the MBT'$_{5me}$ (0.5±0.0) is similar to the Tagus River SPM
355 value (Fig. 3f). The average value of the DC' is 0.3±0.1 and the mean value of the IR is
356 0.5±0.0 (Figs. 3d-e; Table 3).

357 *Lisbon Canyon Head sediments.* The average sum of the brGDGTs, 31±9.3 µg g OC^{-1},
358 is about the same in the Lisbon Canyon Head sediments as in the Mudbelt sediments but the
359 amount of crenarchaeol, 390±130 µg gOC^{-1}, is larger in the Lisbon Canyon Head sediments
360 (Figs. 3a-b; Table 3). This results in lower BIT values (0.1±0.0) than in the Mudbelt

Biogeosciences Discuss., doi:10.5194/bg-2016-146, 2016
Manuscript under review for journal Biogeosciences
Published: 30 May 2016

sediments (Fig. 3c; Table 3). The average brGDGT distribution (Fig. 5f) is fairly similar to that of the Tagus Floodplain and Mudbelt sediments and is relatively constant over the Holocene. The average of the MBT'_{5me} (0.5±0.0) is statistically identical to that in the Mudbelt sediments (Fig. 3f; Table 3). However, the average IR, 0.6±0.0, and DC', 0.4±0.0, are both a bit higher (Figs. 3d-e; Table 3).

Lower Setúbal Canyon sediments. The concentrations of the brGDGTs in these most distal sediments are quite low, on average 16±5.5 µg OC^{-1} (Fig. 3a; Table 3), while the amount of crenarchaeol in this sediment core is the highest out of the entire transect at 470±200 µg gOC^{-1} (Fig. 3b; Table 3). This results in a low average BIT index value of 0.02±0.01 (Fig. 3c; Table 3). The average distribution of brGDGTs in these sediments (Fig. 5g) is different from the marine sediments from the other two sites, with a higher fractional abundance of IIIa'. However, another component with the same molecular ion eluted at around the same time as IIIa' in the Lower Setúbal Canyon sediments (which we determined was not the "mixed 5,6-dimethyl isomer"; cf. Weber et al., 2015), complicating integration and quantification. This indicates that the brGDGT results from these sediments must be interpreted with some caution. The average MBT'_{5me} (0.6±0.1) and DC' (0.4±0.1) are fairly similar to the Lisbon Canyon Head sediments averages but the average IR (0.7±0.0) is the highest of all sediments (Figs. 3d-f; Table 3).

4.3 PCA

In order to determine the variation in the distribution of brGDGTs, we performed principal component analysis (PCA) on the distributions of brGDGTs of all the samples examined. Most variation is explained by principal component 1 (PC1; 29.8 %) and is clearly related to the fractional abundance of the 5-methyl versus 6-methyl brGDGTs (Fig. 6a). With

Biogeosciences Discuss., doi:10.5194/bg-2016-146, 2016
Manuscript under review for journal Biogeosciences
Published: 30 May 2016

the exception of IIIc (which is typically a minor brGDGT with a fractional abundance of <1 %; Fig. 5), all of the 5-methyl brGDGTs score positively on PC1 and the 6-methyl brGDGTs score negatively. For the overall data set, PC1 is highly negatively correlated with the IR ratio (Fig. 7a, R^2=0.78). PC2 explains 25.6 % of the variance of the PCA. Branched GDGTs that score positively on PC2 are generally comprised of cyclized and more methylated brGDGTs (Fig. 6a). With the exception of IIIc (which is typically a minor brGDGT with a fractional abundance of <1 %; Fig. 4), all of the tetra- and penta-methylated brGDGTs containing no cyclopentane moiety (i.e. Ia, IIa, and IIa') score negatively on PC2. Consequently, PC2 is highly positively correlated with DC' for the whole data set (Fig. 7b, R^2=0.84).

4. Discussion

5.1 Environmental parameters affecting brGDGT distribution in Tagus soils

Evident from the earlier study by Zell et al. (2014) was that the distribution of the brGDGTs in Tagus soils varies widely. The primary environmental parameters influencing brGDGT distributions in soil (Weijers et al., 2006), i.e. MAT and pH, did differ substantially in the Tagus River basin. MAT varies from 10-17°C and pH from 5.5-8.6 (Zell et al., 2014) and both parameters show a distinct correlation with altitude (R^2=0.93 and 0.73, respectively). Applying the brGDGT global soil calibration of Peterse et al. (2012), Zell et al. (2014) arrived at unrealistically low (0-10°C) estimated MATs using the brGDGT distributions. This was attributed to the arid conditions in the region (MAP<800 mm yr^{-1}), which has in other studies, including one that analyzed soils from the Iberian peninsula, been indicated as a likely cause for the discrepancy between actual and reconstructed MAT using brGDGT distributions (Peterse et al., 2012; Dirghangi et al., 2013; Menges et al., 2013). Our re-analysis of the soils taking into account the novel 6-methyl brGDGTs now provides the possibility to re-evaluate

Biogeosciences Discuss., doi:10.5194/bg-2016-146, 2016
Manuscript under review for journal Biogeosciences
Published: 30 May 2016

these data. It is clear that the fractional abundances of the novel 6-methyl brGDGTs vary to a large extent. The IR_{II} and IR_{III} vary from 0.1 to 0.9 (Fig. 4) and some of the soils score very negatively on PC1 (Fig. 6b), which is predominantly determined by the fractional abundance of the 6-methyl brGDGTs. From the global soil brGDGT dataset (De Jonge et al., 2014a) it was evident that the main factor influencing the fractional abundance of the 6-methyl brGDGTs is soil pH with an increased abundance in high pH soils. In the Tagus River basin soil pH indeed shows a large variation, i.e. from 5.5 to 8.6, and this likely explains the large variation in IR. When we calculate the pH from the brGDGT distribution using the new equation (9) of De Jonge et al. (2014a), which is based predominantly on the fractional abundances of 6-methyl brGDGTs, we find a highly significant correlation between measured and reconstructed pH (R^2=0.89) following the 1:1 line (Fig. 9a). Differences in soil pH also affect the degree of cyclization of brGDGTs (Weijers et al., 2007a; De Jonge et al., 2014b) and indeed we find a significant positive correlation between DC' and soil pH (R^2=0.74). The effect of MAT is not clearly revealed in the dataset. For the global soil brGDGT dataset a strong relationship exists between MAT and MBT'_{5Me} (De Jonge et al., 2014a). Although we observe substantial variation for MBT'_{5Me} in soils (i.e. 0.3-0.7; Fig. 3f) for this dataset, we do not observe a statistically significant relationship of MAT with MBT'_{5Me}. Also, reconstructed MATs are far too low, i.e. 0.5–13°C using equation (6) and 2.6–11°C using equation (10). Evidently, the "cold bias" of the brGDGT distributions in the soils of the Tagus river basin (Zell et al., 2014) is not solved when 5- and 6-methyl brGDGTs are individually quantified.

Previously it was postulated that in this region aquatic in-situ production and arid conditions are complicating the use of brGDGTs for climate reconstructions (Menges et al., 2013; Zell et al., 2014). Within the soil sample set a strong negative relationship exists between the DC' and the measured MAT in the Tagus basin (R^2=0.79), whereas the degree of cyclization up until this point has only been reported to be related to pH and not to MAT

Biogeosciences Discuss., doi:10.5194/bg-2016-146, 2016
Manuscript under review for journal Biogeosciences
Published: 30 May 2016

(Weijers et al., 2007a). Conversely, though, the MAT_{mrs} reconstructed values for the soils have a positive correlation with DC' (R^2=0.51) and it is lower than with the measured MAT. Although at this point we are unsure if this association occurs in other arid areas as well, we do believe this strong relationship between the DC' and the MAT could be affecting the applicability of brGDGTs for temperature reconstructions in this region.

5.2 Provenance of brGDGTs in the Tagus River and its outflow

The application of brGDGTs in marine sediments influenced by river outflows for reconstruction of the continental paleoclimate (e.g. Weijers et al., 2006) rests on the premise that the distribution of the brGDGTs produced in the soils must be conserved throughout riverine transport to the sediments where they are archived. Therefore, we compare brGDGT distributions and concentrations from the rest of the sample set in the source-to-sink transect to determine if the soil signal is conserved during transport in the Tagus River basin. The PCA results (Fig. 6b) indicate that for the most part the distribution of brGDGTs from the river SPM and sediments along the transect is not similar to those from the soils or the Tagus Watershed. Sediments from three of the sample sets in the transect, the Tagus River Floodplain sediments, the Mudbelt sediments and the Lisbon Canyon Head sediments, all plot differently from the soils, and although the distributions of the Lower Setúbal Canyon sediments and the Tagus River SPM plot closer, there is still an offset from the soils. The Tagus Riverbank sediments plot the most closely to that of the soils in the Tagus River basin, however, again a slight offset still exists. So, even without considering the effects of environmental parameters on brGDGT distributions, we can already conclude that the brGDGTs in the sediments and river SPM only reflect the distribution of brGDGTs in the

Biogeosciences Discuss., doi:10.5194/bg-2016-146, 2016
Manuscript under review for journal Biogeosciences
Published: 30 May 2016

Tagus soils by a minor extent and, thus, it is unlikely that Tagus soils are a major source for brGDGTs in the marine sediments.

Using PCA (Fig. 6) we tried to determine what factors are causing the variation in the distribution of brGDGTs in the Tagus River basin. PC1 is primarily related to the predominance of 5-methyl versus 6-methyl brGDGTs (Fig. 6a) and thus pH (cf. De Jonge et al., 2014a). This was confirmed for the soil data set where the calculated pH based on the fractional abundance of predominantly 6-methyl brGDGTs shows a good correspondence with measured pH (see Sect. 5.1). De Jonge et al. (2014b) showed that in the SPM of the alkaline waters of the river Yenisei 6-methyl brGDGTs also predominate, indicating that pH in all kinds of environmental settings determines the ratio between 5 and 6-methyl brGDGTs. The Tagus riverbank sediments, river SPM and the Lower Setúbal Canyon sediments score mostly negatively on PC1 as do soils from higher altitudes (>350 m) (Fig. 6b). The Mudbelt sediments, Lisbon Canyon Head sediments, the Tagus River Floodplain sediments, and the lower altitude soils (<350 m) have similar abundances of the 5- and 6-methyl brGDGTs or higher abundances of the 5-methyl brGDGTs and plot mostly positively on PC1. Since the Tagus River Floodplain sediments, the Mudbelt sediments, and the Lisbon Canyon Head sediments do not have a predominance of 6-methyl brGDGTs, this indicates that either they received an equal contribution of soil derived organic matter from the lower altitude soils in the region (<350 m) as from the higher altitude region (>350m) or, more likely, that in-situ production of brGDGTs is a large source of brGDGTs in these sample sets.

PC2 also explains a substantial part of the variance in the dataset (25.6 %, Fig. 6b) and is correlated with DC' (R^2=0.84, Fig. 7b). Since pH is also the main driver of DC' (Weijers et al., 2007a), it suggests that differences in pH are also responsible for the variance seen in PC2. The samples that standout are the sediments from the Lower Setúbal Canyon core, which are the most marine sediments in the sample set, and plot most positively, and the

Biogeosciences Discuss., doi:10.5194/bg-2016-146, 2016
Manuscript under review for journal Biogeosciences
Published: 30 May 2016

lowest altitude soils (28-344 m), which plot the most negatively. These latter soils are characterized by a low measured pH. The oldest (11.6-13.0 kys BP) sediments of the Lower Setúbal Canyon score most positively on PC2. A high degree of cyclization of brGDGTs has been observed previously in marine sediments from a Svalbard fjord and attributed to marine in-situ production in the alkaline pore waters of marine sediments (Peterse et al., 2009; Weijers et al, 2014). Re-analysis of the Svalbard sediments for brGDGTs actually showed that this cyclization affects the tetra- and pentamethylated brGDGTs to a much larger extent than that of the hexamethylated brGDGTs (Sinninghe Damsté et al., unpublished results) and the same observation can be made for the sediments of the Lower Setúbal Canyon (Fig. 5g). Evidently, the high degree of cyclization of brGDGTs as a response to pH is not as clearly seen in the soils since the high altitude, high pH soils from the Tagus watershed (Fig. S3c) do not exhibit the pattern (i.e. fractional abundance of IIb' larger than that of IIa') observed in the Lower Setúbal Canyon sediments (Fig. 5g). This pattern is, to a lesser degree, also seen in the sediments of the Lisbon Canyon Head core (Fig. 5f). As mentioned earlier, the Lower Setúbal Canyon sediments also display a predominance of 6-methyl brGDGTs over the 5-methyl counterparts, especially with regards to the hexamethylated brGDGTs. In the Lower Setúbal Canyon sediments IIIa' is by far the most abundant brGDGT, consisting of 29 % of the entire brGDGT pool (Fig. 5g). This is comparable to Svalbard sediments (Sinninghe Damsté et al., unpublished results) where IIIa' is also the most abundant brGDGT. Taken together this clearly indicates the influence of in-situ production in the Lower Setúbal Canyon sediments. However, the degree of cyclization for Ia-c and IIa-c is not as high as observed for the Svalbard sediments, which still suggests some allochthonous input of brGDGTs even in these remote marine sediments.

Another way to determine if in-situ production is a factor affecting the brGDGT distribution in aquatic environments is by the calculation of reconstructed pH values. If in-situ

Biogeosciences Discuss., doi:10.5194/bg-2016-146, 2016
Manuscript under review for journal Biogeosciences
Published: 30 May 2016

production is heavily contributing to the brGDGT pool, then the reconstructed pH values should reflect that of the aquatic environment in which they were produced. The average reconstructed pH of the sample sets in the transect are relatively high with a clear trend to higher values with increasing distance from the river mouth (Fig. 8a), which would be in line with increased in situ production of brGDGTs in the alkaline pore waters of marine sediments. However, these values are still within the range of the measured (5.5-8.5) and reconstructed (Fig. 8a) pH of the soils and so this does not prove in-situ production as a major contributor of brGDGTs in these sample sets. Conversely, the newly calculated DC', also a reflection of pH, is quite variable throughout the sample sets in the transect except for in the river SPM where it is fairly constant (Fig. 3d; Table 3). Since the DC' is lowest in the soils (0.2±0.1) and then higher in the rest of the samples in the transect (0.3-0.4), this suggests in-situ production is an issue (cf. Zell et al., 2014) in all of the sample sets (Fig. 3d; Table 3).

5.3 brGDGTs as indicators of terrestrial OM transport by the Tagus River

Classically, the assessment of the contribution of terrestrial OM to marine sediments is performed by measuring $\delta^{13}C_{TOC}$ (Hedges and Oades, 1997 and references cited therein). In the earlier study of the Tagus River system, Zell et al. (2014) determined that the average $\delta^{13}C_{TOC}$ of the riverine SPM (~-29 ±0.8‰), like the Tagus soils, are consistent with a predominant C_3 higher plants origin (Fry and Sherr, 1984). Additionally, this study found the $\delta^{13}C_{TOC}$ in marine surface sediments off the Portuguese coast in front of the Tagus River increase with increasing distance offshore by an increased contribution of ^{13}C-enriched marine OM. This trend is also evident for the Holocene sediments studied here. The most terrestrial sediments of the transect, i.e. from the Tagus River Floodplain, also have a $\delta^{13}C_{TOC}$ value (~27±1.0 ‰; Fig. 2a; Table 3) consistent with a predominant C_{origin} of higher plants.

Biogeosciences Discuss., doi:10.5194/bg-2016-146, 2016
Manuscript under review for journal Biogeosciences
Published: 30 May 2016

531 Moving offshore, the less negative $\delta^{13}C_{TOC}$ values of the Mudbelt sediments (-24±0.2 ‰), the
532 Lisbon Canyon Head sediments (-23±0.6 ‰) and the Lower Setúbal Canyon sediments (-
533 23±1.5 ‰) all indicate that the majority of the TOC off the Portuguese shelf is of marine
534 origin (Fig. 2a; Table 3). So, as Zell et al. (2014) found with marine surface sediments off the
535 Portuguese coast, the $\delta^{13}C_{TOC}$ (‰) averages from the sediments in our transect also increase
536 with increasing distance offshore, demonstrating that the present trend in the $\delta^{13}C_{TOC}$ signal
537 remained the same over the Holocene.

538 Zell et al. (2014) previously showed that in the present day Tagus River system the
539 amount of brGDGTs (µg gOC^{-1}) increases from the soils to the riverbank sediment to the river
540 SPM and explained this increase as proof of riverine in-situ production of brGDGTs.
541 Concentrations of summed brGDGTs in surface sediments in transects from the Portuguese
542 coast rapidly declined with increasing distance from the coast, suggesting that brGDGTs
543 could still be used as tracer for terrestrial organic matter (Zell et al., 2015). The trends
544 observed in these earlier studies are confirmed here for the Holocene. The Tagus River
545 Floodplain sediments have the highest concentration of brGDGTs (67±26 µg gOC^{-1}) in the
546 entire transect, much higher than in the soils (Fig. 3b; Table 3). However, the sediments in
547 this core are somewhat a-typical for the Tagus Floodplain as some layers consist of peat as a
548 result of the low-energy backswamp conditions in the vicinity, which could explain the
549 difference in brGDGT concentrations from the surrounding soils. This could also be due to
550 the addition of aquatically produced brGDGTs from the river during times of flooding
551 although it should be noted that the concentration of brGDGTs is even higher than in riverine
552 SPM (Fig. 3b). The summed brGDGT concentration decreases and is fairly similar among the
553 Mudbelt sediments (25±14 µg gOC^{-1}) and the Lisbon Canyon Head sediments (31±9.3 µg
554 gOC^{-1}), and then decreases further moving away from the coastline to the Lower Setúbal
555 Canyon sediments (16±5.5 µg gOC^{-1}) demonstrating the decrease in input of riverine

Biogeosciences Discuss., doi:10.5194/bg-2016-146, 2016
Manuscript under review for journal Biogeosciences
Published: 30 May 2016

556 brGDGTs moving away from the shoreline (Fig. 3b). However, even though the sum of the
557 brGDGTs are lower in the marine sediment than in the Tagus River Floodplain sediments, the
558 amount of brGDGTs in all four sediment cores are higher than in the Tagus soils (~6.8±6.5 µg
559 gOC^{-1}) indicating the origin of the brGDGTs in the sediment cores are not all soil derived and
560 pointing instead to riverine in-situ production as well as possibly in aquatic sediments (Fig.
561 3b).

562 A previous study by Zell et al., (2015) determined that in the surface sediments off the
563 coast of Portugal the BIT index is influenced by both declining brGDGT concentrations and
564 increased crenarchaeol production with increasing distance from the coast. For the Holocene
565 sediments studied here, the average concentration of crenarchaeol in the Tagus River
566 Floodplain sediments is low (2.8±1.7 µg gOC^{-1}) and similar to that of the Tagus soils (1.4±1.1
567 µg gOC^{-1}; Fig. 3a; Table 3). The crenarchaeol concentration increases in the sediments with
568 increasing distance from the shoreline, signifying the increase in marine production with
569 water depth and distance from the coast (Fig. 3a). Consequently, the BIT index is the highest
570 in the Tagus River Floodplain sediments (0.94±0.03) out of the entire transect (Fig. 3c) and
571 then the BIT index decreases within the sediments along the transect with increasing distance
572 from the Portuguese coast potentially signifying a decrease in terrestrial input moving away
573 from the shoreline. A moderate negative correlation exists between the BIT index and $\delta^{13}C_{TOC}$
574 values for the entire sample set (R^2=0.55, Fig. 10), demonstrating that as $\delta^{13}C_{TOC}$ values
575 become less terrestrial, the BIT index indicates less terrestrial input, so both parameters
576 corroborate a decrease in terrestrial influence with distance from the coast confirming the
577 results from previous studies (Zell et al., 2014; 2015).

578

Biogeosciences Discuss., doi:10.5194/bg-2016-146, 2016
Manuscript under review for journal Biogeosciences
Published: 30 May 2016

579 **5.4 Factors affecting the application of brGDGTs for paleoclimate reconstructions off**
580 **the Iberian Peninsula**

581 Despite the caveats with respect to in-situ production of brGDGTs in aquatic
582 environments as described in the previous section, we tested how the new soil calibration
583 based on individually quantified 5-methyl and 6-methyl brGDGTs (De Jonge et al., 2014a)
584 performed to reconstruct continental MAT in this region. For this comparison we will
585 consider the present day MAT of the entire Tagus River basin, 14.6±2.2°C (Zell et al., 2014),
586 assuming that soil derived brGDGTs from along the whole river basin are contributing to the
587 marine sediments. The assumption that the brGDGTs from the entire Tagus River basin are
588 being contributed to oceanic sediments is probably invalid for modern times as the
589 construction of dams along the Tagus River, which began in the 1940s, most likely prevents
590 part of the terrestrial material from upstream making it downstream and out off the coast of
591 Portugal. However, since we are not looking at marine surface sediments in this study but
592 instead sediments deposited during the Holocene, the placement of dams in the river should
593 not affect our results except for with the riverine SPM. Despite the separation of the 5- and 6-
594 methyl brGDGT isomers and the application of the new proxy, the reconstructed MATs using
595 both riverine SPM and Holocene sediments is still substantially lower than 14.6°C (Figs. 8b
596 and 8c), as noted for the soils (see Sect. 5.1). Using the MAT_{mr} calibration the Lisbon Canyon
597 Head sediments the average temperature (12.4±0.5°C) comes closest to the modern day MAT
598 in the region and using the MAT_{mrs} calibration the Lower Setúbal Canyon sediments
599 (11.2±0.7°C) has the most similar average temperature (Figs. 8b and 8c).

600 Even though we used the new calibration to reconstruct MAT, it should be noted that
601 the low BIT values (<0.15; Fig. 3c) of the Holocene sediments deposited at the three marine
602 sites indicates that there were probably not enough soil-derived brGDGTs making it out to
603 ocean and being deposited in the sediments over the Holocene for reliable climate

Biogeosciences Discuss., doi:10.5194/bg-2016-146, 2016
Manuscript under review for journal Biogeosciences
Published: 30 May 2016

reconstructions (cf. Weijers et al., 2014). By looking at the summed concentration of brGDGTs along the entire transect, it is apparent that since it is lowest in the soils that although the BIT index seems high enough for MAT reconstructions in the riverbank sediments and river SPM, the origin of the brGDGTs may not be solely soil derived and this could be complicating reconstructions throughout the transect as was discussed previously (see Sect. 5.2). This further supports earlier conclusions from preceding studies (Yang et al., 2012; Zell et al., 2013) stating that the amount and origin of brGDGTs in a system needs to be examined along with the BIT index when determining if brGDGTs can be applied for MAT reconstruction.

6. Conclusions

We have established that the distribution of brGDGTs varies greatly within the Tagus River basin (Fig. 5) and although this may be partly explained by the varying contributions of higher altitude, which contain a greater proportion of 6-methyl isomers, versus lower altitude soils in the sample sets it is more likely due to the contribution of aquatically produced brGDGTs in some of the sample sets. In order to use sedimentary brGDGTs for paleoclimate reconstructions, the distribution of brGDGTs in the soils must be related to the MAT and conserved throughout riverine transport to the sediments where they are deposited, however, our results corroborate previous studies stating that most of the terrestrial matter is not making it out to the ocean and being deposited in sediments close to shore. The lack of soil derived OM in offshore sediments along with the substantial input of aquatically produced brGDGTs is complicating MAT reconstructions from sedimentary, marine brGDGTs in this region.

Additionally, we confirm the findings of Zell et al., (2014; 2015) that in-situ production of brGDGTs is occurring in the river and marine systems of the Tagus River basin and go on

Biogeosciences Discuss., doi:10.5194/bg-2016-146, 2016
Manuscript under review for journal Biogeosciences
Published: 30 May 2016

628 to show that there are indications that it occurred in the past as well. Although in-situ
629 production is complicating environmental reconstructions using marine sediments, another
630 issue is that accurate MAT reconstructions using brGDGTs cannot currently be performed on
631 the soils, even with the separation of the 6-methyl brGDGTs from the 5-methyl isomers using
632 the new method and calibrations. Previous studies have concluded that paleoclimate
633 reconstructions in arid regions using brGDGTs are complicated due to a breakdown in the
634 relationship with MBT' and MAT (Peterse et al., 2012; Menges et al., 2013). In this study we
635 confirm that there is not a strong relationship between the MBT'$_{5me}$ and measured MAT in
636 this arid region. However, we also do not observe the same relationship with MAP and
637 MBT'$_{5me}$ that has been previously reported between MAP and MBT' in arid regions and has
638 been implicated in making reconstructions difficult. Instead, we see a strong relationship with
639 the DC' and measured MAT in the area not observed before. We also see a predominance of
640 6-methyl isomers, previously only reported in river SPM, in the Tagus soils from greater than
641 350 m altitude. Although this might be a characteristic of arid soils and related to MAP since
642 it is below 550 mm yr^{-1} in most of the soil samples above 350 m, the two highest elevation
643 soil samples, which both have a MAP above 550 mm yr^{-1}, also demonstrate this trend. Future
644 studies need to be performed in arid environments to determine if a strong relationship
645 between MAT and DC' as well as a predominance of 6-methyl isomers are characteristics of
646 arid regions and contributing to the complications found using brGDGTs for paleoclimate
647 reconstructions. Also, higher elevation environments should be further studied to determine if
648 a predominance of 6-methyl brGDGTs is a feature of higher altitudes and complicating
649 climate reconstructions.

650 Because of these unique features in this region, perhaps the development of a local
651 calibration could assuage difficulties in using brGDGTs as a paleoclimate proxy for soils in
652 the Tagus River basin. This would not, however, solve the issue of in-situ produced brGDGTs

Biogeosciences Discuss., doi:10.5194/bg-2016-146, 2016
Manuscript under review for journal Biogeosciences
Published: 30 May 2016

overwhelming the amount of soil derived brGDGTs in aquatic sediments. We did find that the new CBT' and pH calibration do an excellent job reconstructing pH in the soils of the Tagus basin and since pH is related to other environmental factors such as MAP this will be useful for paleoclimate reconstructions in terrestrial sites over the Iberian peninsula where in-situ production is not a complicating factor.

Author contribution

J.H. Kim and J.S.S. Damsté designed the study which was carried out by L. Warden who completed bulk carbon isotope and brGDGT analysis on samples along with C. Zell. C. Zell, H. Stigter, G.J. Vis and J.H. Kim collected samples for this study. J. Bonnin picked forams for dating. L. Warden and J.S.S. Damsté prepared the manuscript with contributions from all co-authors.

Acknowledgements

The research leading to these results has received funding from the European Research Council under the European Union's Seventh Framework Programme (FP7/2007-2013) / ERC grant agreement n° [226600]. JSSD is supported by funding from the Netherlands Earth System Science Center (NESSC) though a gravitation grant from the Dutch ministry for Education, Culture and Science. We thank the captain and crew of the R/V Pelagia for their support with sampling. We thank J. Ossebaar and E.C. Hopmans for their help with the HPLC-APCI-MS analysis, J. Ossebaar for his help with the element analyzer, and L.A.C. Rosales and A. Mets for help with sample preparation.

Biogeosciences Discuss., doi:10.5194/bg-2016-146, 2016
Manuscript under review for journal Biogeosciences
Published: 30 May 2016

676 **Data Availability**

677 The data presented in this paper can be found in Table 3.

678 **Figure captions**

679 **Figure 1** The location of the study area on the Iberian Peninsula with the stations where the
680 four sediment cores were sampled (indicated by black squares) along a transect from the
681 Tagus River to off the Portuguese continental margin as well as the river SPM sampling site
682 (indicated by a white diamond), riverbank sediment sampling sites (indicated by red circles),
683 and soil sampling sites (indicated by black circles). The River SPM, riverbank sediments and
684 soil samples were all collected for a previous study. Digital elevation data from Jarvis et al.
685 (2006) and bathymetry from IOC-IHO-BODC (2003).

686 **Figure 2** Boxplots of (a) $\delta^{13}C_{TOC}$ (‰) of the organic carbon and (b) TOC (wt. %) for each
687 sample set along the Tagus River source to sink transect. The increasing $\delta^{13}C_{TOC}$ values in the
688 sediment core locations with increasing distance from the coast indicates that more of the
689 organic carbon in these sediments is marine derived.

690 **Figure 3** Boxplots of (a) crenarchaeol concentrations (µg gOC^{-1}), (b) sum of brGDGTs (µg
691 gOC^{-1}), (c) BIT index, (d) DC', (e) IR, (f) MBT'_{5me} for each sample set in the transect from
692 the land to the ocean off the Portuguese coast.

693 **Figure 4** Isomer ratio for the non-cyclized pentamethylated brGDGT (IR_{II}) plotted against
694 that of the non-cyclized hexamethylated brGDGT (IR_{III}).

695 **Figure 5** Average distribution of brGDGTs for each sample set along the transect of samples
696 that runs from the land to the ocean off the coast of Lisbon. Evident from this figure is that the
697 distribution of brGDGTs within this sample set varies greatly. Distributions of brGDGTs in
698 marine sediments only reflects the distribution of the brGDGTs from the Tagus soils to a

Biogeosciences Discuss., doi:10.5194/bg-2016-146, 2016
Manuscript under review for journal Biogeosciences
Published: 30 May 2016

699 minor extent. The color of the bars reflects the brGDGT structure as labeled in the legend and
700 the range indicated with the error bars equals 2xs the standard deviation.

701 **Figure 6** Principal component analysis based on the fractional abundances of the 15
702 brGDGTs of samples in the transect that runs from inland to off the coast of Portugal plotting
703 a) the scores of the brGDGT compounds on the first two principal components (PC) and b)
704 the scores of the samples from each sample set used in this study.

705 **Figure 7** Scatter plots of (a) PC1 against the IR (R^2=0.78) and (b) PC2 against DC' (R^2=0.84)
706 for the entire set of samples used in this study.

707 **Figure 8** Boxplots of all the sample sets within the transect from the land to the deep ocean
708 off the Portuguese coast for (a) reconstructed pH, (b) MAT_{mrs} (°C) and (c) MAT_{mr} (°C). Red
709 dotted line indicates estimated present day MAT for the Tagus River basin (14.6°C).

710 **Figure 9** Panels a-c show scatterplots of the Tagus soil samples for a) reconstructed and
711 measure pH (R^2=0.89), b) reconstructed MAT_{mr} (°C) and measured MAT (°C) (R^2=0.27), c)
712 reconstructed MAT_{mrs} (°C) and measured MAT (°C) (R^2=0.38). For panels b-c the soil
713 samples from an altitude greater than 350m are indicated in black and those from an altitude
714 below 350m are indicated in green. Panels d-f show scatter plots of the Tagus riverbank
715 sediments for d) reconstructed and measured pH (R^2=0.14), e) reconstructed MAT_{mr} (°C) and
716 measured MAT (°C) (R^2=0.31), f) reconstructed MAT_{mrs} (°C) and measured MAT (°C)
717 (R^2=0.23). Panel g is a scatter plot showing the reconstructed and measured pH for the Tagus
718 River SPM samples (R^2=0.09).

719 **Figure 10** Scatterplot of the BIT index and $\delta^{13}C_{TOC}$ (‰ VPDB) for the entire Portuguese
720 sample set (R^2=0.55). In general, higher BIT values correlate with more depleted $\delta^{13}C_{TOC}$
721 indicating a more terrestrial signal and lower BIT values correlate with less depleted $\delta^{13}C_{TOC}$
722 indicating a more marine signal.

Biogeosciences Discuss., doi:10.5194/bg-2016-146, 2016
Manuscript under review for journal Biogeosciences
Published: 30 May 2016

723

724 **References**

725 Abrantes, F., Lebreiro, S., Rodrigues, T., Gil, I., Bartels-Jónsdóttir, H., Oliveira, P., Kissel,
726 C., and Grimalt, J.O.: Shallow-marine sediment cores record climate variability and
727 earthquake activity off Lisbon (Portugal) for the last 2000 years, Quat. Sci. Rev., 24, 2477–
728 2494, 2005.

729 Abrantes, F., Lopes, C., Rodrigues, T., Gil, I., Witt, L., Grimalt, J., and Harris, I.: Proxy
730 calibration to instrumental data set: Implications for paleoceanographic reconstructions,
731 Geochem. Geophy. Geosy., 10, Q09U07, doi:10.1029/2009GC002604, 2009.

732 Andreu, L., GutiéRrez, E., Macias, M., Ribas, M., Bosch, O., and Camarero, J.J.: Climate
733 increases regional tree-growth variability in Iberian pine forests, Glob. Change Biol., 13, 1-
734 12, 2007.

735 Bartels-Jónsdóttir, H.B., Knudsen, K.L., Abrantes, F., Lebreiro, S., and Eiríksson, J.: Climate
736 variability during the last 2000 years in the Tagus Prodelta, western Iberian Margin: Benthic
737 foraminifera and stable isotopes, Mar. Micropaleontol., 59, 83–103, 2006.

738 Bartels-Jonsdottir, H.B., Voelker, A.H.L., Knudsen, K.L., and Abrantes, F.: Twentieth-
739 century warming and hydrographical changes in the Tagus Prodelta, eastern North Atlantic,
740 Holocene, 19, 369–380, 2009.

741 Bendle, J.A., Weijers, J.W., Maslin, M.A., Sinninghe Damsté, J.S., Schouten, S., Hopmans,
742 E.C., Boot, C.S., and Pancost, R.D.: Major changes in glacial and Holocene terrestrial
743 temperatures and sources of organic carbon recorded in the Amazon fan by tetraether lipids,
744 Geochem. Geophy. Geosy., 11, Q12007, doi:10.1029/2010GC003308, 2010.

745 Benito, G., Díez-Herrero, A., and de Villalta, M.F.: Magnitude and frequency of flooding in
746 the Tagus basin (Central Spain) over the last millennium, Climatic Change, 58, 171–192,
747 2003.

748 Cachao, M., and Moita, M.T.: *Coccolithus pelagicus,* a productivity proxy related to moderate
749 fronts off Western Iberia, Mar. Micropaleontol, 39, 131–155, 2000.

750 Corella, J.P., Stefanova, V., El Anjoumi, A., Rico, E., Giralt, S., Moreno, A., Plata-Montero,
751 A., and Valero-Garcés, B.L.: A 2500-year multi-proxy reconstruction of climate change and
752 human activities in northern Spain: The Lake Arreo record, Palaeogeogr. Palaeoecol., 386,
753 555–568, 2013.

754 Damsté, J.S.S., Schouten, S., Hopmans, E.C., van Duin, A.C., and Geenevasen, J.A.:
755 Crenarchaeol the characteristic core glycerol dibiphytanyl glycerol tetraether membrane lipid
756 of cosmopolitan pelagic crenarchaeota, J. Lipid Res., 43, 1641–1651, 2002.

757 Damste, J.S.S., Ossebaar, J., Abbas, B., Schouten, S., and Verschuren, D.: Fluxes and
758 distribution of tetraether lipids in an equatorial African lake: Constraints on the application of
759 the TEX_{86} palaeothermometer and BIT index in lacustrine settings, Geochim. Cosmochim.
760 Ac., 73, 4232–4249, 2009.

Biogeosciences Discuss., doi:10.5194/bg-2016-146, 2016
Manuscript under review for journal Biogeosciences
Published: 30 May 2016

761 Damste, J.S.S., Rijpstra, W.I.C., Hopmans, E.C., Weijers, J.W.H., Foesel, B.U., Overmann,
762 J., and Dedysh, S.N.: 13,16-Dimethyl Octacosanedioic Acid (iso-Diabolic Acid), a Common
763 Membrane-Spanning Lipid of Acidobacteria Subdivisions 1 and 3, Appl. Environ. Microb.,
764 77, 4147–4154, 2011.

765 Damsté, J.S.S., Rijpstra, W.I.C., Hopmans, E.C., Foesel, B.U., Wüst, P.K., Overmann, J.,
766 Tank, M., Bryant, D.A., Dunfield, P.F., Houghton, K. and Stott, M.B.: Ether- and Ester-
767 Bound iso-Diabolic Acid and Other Lipids in Members of Acidobacteria Subdivision 4, Appl.
768 Environ. Microb., 80, 5207–5218, 2014.

769 Davis, B.A.S., Brewer, S., Stevenson, A.C., and Guiot, J.: The temperature of Europe during
770 the Holocene reconstructed from pollen data, Quaternary Sci. Rev., 22, 1701–1716, 2003.

771 De Jonge, C., Hopmans, E.C., Stadnitskaia, A., Rijpstra, W.I.C., Hofland, R., Tegelaar, E.,
772 and Damsté, J.S.S.: Identification of novel penta-and hexamethylated branched glycerol
773 dialkyl glycerol tetraethers in peat using HPLC–MS 2, GC–MS and GC–SMB-MS. Org.
774 Geochem., 54, 78–82, 2013.

775 De Jonge, C., Hopmans, E.C., Zell, C.I., Kim, J.-H., Schouten, S., and Damsté, J.S.S.:
776 Occurrence and abundance of 6-methyl branched glycerol dialkyl glycerol tetraethers in soils:
777 Implications for palaeoclimate reconstruction. Geochim. Cosmochim. Ac., 141, 97–112,
778 2014a.

779 De Jonge, C., Stadnitskaia, A., Hopmans, E.C., Cherkashov, G., Fedotov, A., and Damsté,
780 J.S.S.: In situ produced branched glycerol dialkyl glycerol tetraethers in suspended particulate
781 matter from the Yenisei River, Eastern Siberia, Geochim. Cosmochim. Ac., 125, 476–491,
782 2014b.

783 De Jonge, C., Stadnitskaia, A., Hopmans, E.C., Cherkashov, G., Fedotov, A., Streletskaya,
784 I.D., Vasiliev, A.A., and Damsté, J.S.S.: Drastic changes in the distribution of branched
785 tetraether lipids in suspended matter and sediments from the Yenisei River and Kara Sea
786 (Siberia): Implications for the use of brGDGT-based proxies in coastal marine sediments,
787 Geochim. Cosmochim. Ac., 165, 200-225, 2015.

788 Dias, J.M.A., Jouanneau, J.M., Gonzalez, R., Araújo, M.F., Drago, T., Garcia, C., Oliveira,
789 A., Rodrigues, A., Vitorino, J., and Weber, O.: Present day sedimentary processes on the
790 northern Iberian shelf, Prog. Oceanogr., 52, 249–259, 2002.

791 Dirghangi, S.S., Pagani, M., Hren, M.T., and Tipple, B.J.: Distribution of glycerol dialkyl
792 glycerol tetraethers in soils from two environmental transects in the USA, Org. Geochem., 59,
793 49–60, 2013.

794 Fletcher, W.J., Boski, T., and Moura, D.: Palynological evidence for environmental and
795 climatic change in the lower Guadiana valley, Portugal, during the last 13, 000 years,
796 Holocene, 17, 481–494, 2007.

797 Fry, B., and Sherr, E.: δ13C measurements as indicators of carbon flow in marine and
798 freshwater ecosystems, Contrib. Mar. Sci., 27, 15–47, 1984.

799 Haug, G.H., Günther, D., Peterson, L.C., Sigman, D.M., Hughen, K.A., and Aeschlimann, B.:
800 Climate and the collapse of Maya civilization, Science, 299, 1731–1735, 2003.

Biogeosciences Discuss., doi:10.5194/bg-2016-146, 2016
Manuscript under review for journal Biogeosciences
Published: 30 May 2016

Hedges, J.I., and Oades, J.M.: Comparative organic geochemistries of soils and marine sediments, Org. Geochem., 27, 319–361, 1997.

Hopmans, E.C., Schouten, S., and Damsté, J.S.S.: The effect of improved chromatography on GDGT-based palaeoproxies, Org. Geochem., 93, 1-6, 2015.

Hren, M.T., Pagani, M., Erwin, D.M., and Brandon, M: Biomarker reconstruction of the early Eocene paleotopography and paleoclimate of the northern Sierra Nevada, Geology, 38, 7–10, 2010.

Huguet, C., Hopmans, E.C., Febo-Ayala, W., Thompson, D.H., Damsté, J.S.S., and Schouten, S.: An improved method to determine the absolute abundance of glycerol dibiphytanyl glycerol tetraether lipids, Org. Geochem., 37, 1036–1041, 2006.

Huntley, B., and Prentice, I.C.: July Temperatures in Europe from Pollen Data, 6000 Years Before Present, Science, 241, 687–690, 1988.

Hurrell, J.W.: Decadal trends in the North Atlantic oscillation, Science, 269, 676–679, 1995.

Hurrell, J.W., and Van Loon, H: Decadal variations in climate associated with the north Atlantic oscillation. Climatic Change, 36, 301–326, 1997.

International Ocean Commission, International Hydrographic Organization, and British Oceanographic Data Centre (IOC/IHO/BODC): Centenary Edition of the GEBCO Digital Atlas, Published on CD-ROM on Behalf of the Intergovernmental Oceanographic Commission and the International Hydrographic Organization as part of the General Bathymetric Chart of the Oceans, British-Oceanographic-Data-Centre (Ed.), Liverpool, United Kingdom, 2003.

Jarvis, A., Reuter, H.I., Nelson, A., Guevara, E.: Hole-filled seamless SRTM data vol. 3, International Centre for Tropical Agriculture (CIAT), 2006.

Jesus, C.C., de Stigter, H.C., Richter, T.O., Boer, W., Mil-Homens, M., Oliveira, A., and Rocha, F.: Trace metal enrichments in Portuguese submarine canyons and open slope: anthropogenic impact and links to sedimentary dynamics, Mar. Geol., 271, 72–83, 2010.

Jouanneau, J.M., Garcia, C., Oliveira, A., Rodrigues, A., Dias, J.A., and Weber, O.: Dispersal and deposition of suspended sediment on the shelf off the Tagus and Sado estuaries, SW Portugal. Prog. Oceanogr. 42, 233–257, 1998.

Keating-Bitonti, C.R., Ivany, L.C., Affek, H.P., Douglas, P., and Samson, S.D.: Warm, not super-hot, temperatures in the early Eocene subtropics, Geology, 39, 771–774, 2011.

Lastras, G., Arzola, R.G., Masson, D.G., Wynn, R.B., Huvenne, V.A.I., Hühnerbach, V., and Canals, M.: Geomorphology and sedimentary features in the Central Portuguese submarine canyons, Western Iberian margin, Geomorphology, 103, 310–329, 2009.

Lebreiro, S.M., Francés, G., Abrantes, F.F.G., Diz, P., Bartels-Jónsdóttir, H.B., Stroynowski, Z.N., Gil, I.M., Pena, L.D., Rodrigues, T., and Jones, P.D.: Climate change and coastal hydrographic response along the Atlantic Iberian margin (Tagus Prodelta and Muros Ría) during the last two millennia, Holocene, 16, 1003–1015, 2006.

839 Le Pera, E., and Arribas, J.: Sand composition in an Iberian passive-margin fluvial course: the
840 Tajo River, Sediment Geol., 171, 261–281, 2004.

841 Linan, I.D., Gutierrez, E., Andreu-Hayles, L., Heinrich, I., and Helle, G.: Potential to explain
842 climate from tree rings in the south of the Iberian Peninsula, Clim. Res., 55, 119–134, 2012.

843 Martin-Chivelet, J., Belen Munoz-Garcia, M., Edwards, R.L., Turrero, M.J., and Ortega, A.I.:
844 Land surface temperature changes in Northern Iberia since 4000 yr BP, based on delta C-13
845 of speleothems, Glob. Planet Change, 77, 1–12, 2011.

846 Menges, J., Huguet, C., Alcañiz, J.M., Fietz, S., Sachse, D., and Rosell-Melé, A.: Water
847 availability determines branched glycerol dialkyl glycerol tetraether distributions in soils of
848 the Iberian Peninsula, Biogeosciences Disc., 10, 9043–9068, 2013.

849 Munoz-Garcia, M.B., Martin-Chivelet, J., Rossi, C., Ford, D.C., and Schwarcz, H.P.:
850 Chronology of termination II and the Last Interglacial Period in North Spain based on stable
851 isotope records of stalagmites from Cueva del Cobre (Palencia), J. Iber. Geol., 33, 17–30,
852 2007.

853 Palumbo, E., Flores, J.A., Perugia, C., Emanuele, D., Petrillo, Z., Rodrigues, T., Voelker,
854 A.H., and Amore, F.O.: Abrupt variability of the last 24 ka BP recorded by coccolithophore
855 assemblages off the Iberian Margin (core MD03-2699), J. Quaternary Sci., 28, 320–328,
856 2013.

857 Pancost, R.D., and Sinninghe Damsté, J.S.: Carbon isotopic compositions of prokaryotic
858 lipids as tracers of carbon cycling in diverse settings, Chem. Geol., 195, 29–58, 2003.

859 Peterse, F., Kim, J.-H., Schouten, S., Kristensen, D.K., Ko\cc, N., and Damsté, J.S.S.:
860 Constraints on the application of the MBT/CBT palaeothermometer at high latitude
861 environments (Svalbard, Norway), Org. Geochem., 40, 692–699, 2009.

862 Peterse, F., Meer, J. van der, Schouten, S., Weijers, J.W., Fierer, N., Jackson, R.B., Kim, J.-
863 H., and Damsté, J.S.S.: Revised calibration of the MBT-CBT paleotemperature proxy based
864 on branched tetraether membrane lipids in surface soils, Geochim. Cosmochim. Ac., 96, 215-
865 229, 2012.

866 Reimer, P.J., Bard, E., Bayliss, A., Beck, J.W., Blackwell, P.G., Ramsey, C.B., Buck, C.E.,
867 Cheng, H., Edwards, R.L., Friedrich, M. and Grootes, P.M. : IntCal13 and Marine13
868 radiocarbon age calibration curves 0-50,000 years cal BP, Radiocarbon, 55, 1869-1887 2013.

869 Rodó, X., Baert, E., and Comín, F.A.: Variations in seasonal rainfall in Southern Europe
870 during the present century: relationships with the North Atlantic Oscillation and the El Niño-
871 Southern Oscillation, Clim. Dynam., 13, 275–284, 1997.

872 Rodrigues, T., Grimalt, J.O., Abrantes, F.G., Flores, J.A., and Lebreiro, S.M.: Holocene
873 interdependences of changes in sea surface temperature, productivity, and fluvial inputs in the
874 Iberian continental shelf (Tagus mud patch), Geochem. Geophy. Geosystems, 10, Q07U06,
875 doi:10.1029/2008GC002367, 2009.

876 Schouten, S., Eldrett, J., Greenwood, D.R., Harding, I., Baas, M., and Damsté, J.S.S.: Onset
877 of long-term cooling of Greenland near the Eocene-Oligocene boundary as revealed by
878 branched tetraether lipids, Geology, 36, 147–150, 2008.

de Stigter, H.C., Jesus, C.C., Boer, W., Richter, T.O., Costa, A., and van Weering, T.C.: Recent sediment transport and deposition in the Lisbon–Setúbal and Cascais submarine canyons, Portuguese continental margin, Deep-Sea Res. Pt. II, 58, 2321–2344, 2011.

Stoll, H.M., Moreno, A., Mendez-Vicente, A., Gonzalez-Lemos, S., Jimenez-Sanchez, M., Jose Dominguez-Cuesta, M., Edwards, R.L., Cheng, H., and Wang, X.: Paleoclimate and growth rates of speleothems in the northwestern Iberian Peninsula over the last two glacial cycles, Quaternary Res., 80, 284–290, 2013.

Stuiver, M., Reimer, P., and Braziunas, T.: High-precision radiocarbon age calibration for terrestrial and marine samples, Radiocarbon, 40, 1127–1151, 1998.

Trigo, R.M., Pozo-Vazquez, D., Osborn, T.J., Castro-Diez, Y., Gamiz-Fortis, S., and Esteban-Parra, M.J.: North Atlantic oscillation influence on precipitation, river flow and water resources in the Iberian peninsula, Int. J. Climatol., 24, 925–944, 2004.

Vale, C., and Catarino, F.: Accumulation of Zn, Pb, Cu, Cr and Ni in sediments between roots of the Tagus estuary salt marshes, Portugal, Estuar. Coast Shelf S., 42, 393–403, 1996.

Vaz, N., Mateus, M., and Dias, J.M.: Semidiurnal and spring-neap variations in the Tagus Estuary: Application of a process-oriented hydro-biogeochemical model, J. Coastal. Res., 64, 1619–1623, 2011.

Vis, G.-J., and Kasse, C.: Late Quaternary valley-fill succession of the Lower Tagus Valley, Portugal, Sediment Geol., 221, 19–39, 2009.

Vis, G.-J., Kasse, C., and Vandenberghe, J.: Late Pleistocene and Holocene palaeogeography of the Lower Tagus Valley (Portugal): effects of relative sea level, valley morphology and sediment supply, Quat. Sci. Rev., 27, 1682–1709, 2008.

Vis, G.-J., Kasse, C., Kroon, D., Vandenberghe, J., Jung, S., Lebreiro, S.M., and Rodrigues, T.: Time-integrated 3D approach of late Quaternary sediment-depocenter migration in the Tagus depositional system: From river valley to abyssal plain, Earth-Sci. Rev., (in press) 2016.

Weber, Y., De Jonge, C., Rijpstra, W.I.C., Hopmans, E.C., Stadnitskaia, A., Schubert, C.J., Lehmann, M.F., Sinninghe Damsté, J.S., and Niemann, H.: Identification and carbon isotope composition of a novel branched GDGT isomer in lake sediments: Evidence for lacustrine branched GDGT production, Geochim. Cosmochim. Ac., 154, 118-129, 2015.

Weijers, J.W., Schouten, S., Hopmans, E.C., Geenevasen, J.A., David, O.R., Coleman, J.M., Pancost, R.D., and Sinninghe Damsté, J.S.: Membrane lipids of mesophilic anaerobic bacteria thriving in peats have typical archaeal traits. Environ. Microbiol., 8, 648–657, 2006.

Weijers, J.W., Schouten, S., van den Donker, J.C., Hopmans, E.C., and Sinninghe Damsté, J.S.: Environmental controls on bacterial tetraether membrane lipid distribution in soils, Geochim. Cosmochim. Ac., 71, 703–713, 2007a.

Weijers, J.W., Schefuß, E., Schouten, S., and Damsté, J.S.S.: Coupled thermal and hydrological evolution of tropical Africa over the last deglaciation, Science, 315, 1701–1704, 2007b.

Weijers, J.W.H., Wiesenberg, G.L.B., Bol, R., Hopmans, E.C., and Pancost, R.D.: Carbon isotopic composition of branched tetraether membrane lipids in soils suggest a rapid turnover and a heterotrophic life style of their source organism(s), Biogeosciences, 7, 2959–2973, 2010.

Weijers, J.W.H., Bernhardt, B., Peterse, F., Werne, J.P., Dungait, J.A.J., Schouten, S., and Damste, J.S.S.: Absence of seasonal patterns in MBT-CBT indices in mid-latitude soils, Geochim. Cosmochim. Ac., 75, 3179–3190, 2011.

Xie, S., Pancost, R.D., Chen, L., Evershed, R.P., Yang, H., Zhang, K., Huang, J., and Xu, Y.: Microbial lipid records of highly alkaline deposits and enhanced aridity associated with significant uplift of the Tibetan Plateau in the Late Miocene, Geology, 40, 291–294, 2012.

Yang, G., Zhang, C.L., Xie, S., Chen, Z., Gao, M., Ge, Z., and Yang, Z.: Microbial glycerol dialkyl glycerol tetraethers from river water and soil near the Three Gorges Dam on the Yangtze River, Org. Geochem., 56, 40-50, 2013.

Zell, C., Kim, J.-H., Moreira-Turcq, P., Abril, G., Hopmans, E.C., Bonnet, M.-P., Sobrinho, R.L., and Damsté, J.S.S.: Disentangling the origins of branched tetraether lipids and crenarchaeol in the lower Amazon River: Implications for GDGT-based proxies, Limnol. Oceanogr., 58, 343–353, 2013.

Zell, C., Kim, J.-H., Balsinha, M., Dorhout, D., Fernandes, C., Baas, M., and Damsté, J.S.S.: Transport of branched tetraether lipids from the Tagus River basin to the coastal ocean of the Portuguese margin: consequences for the interpretation of the MBT'/CBT paleothermometer, Biogeosciences, 11, 5637–5655, 2014.

Zell, C., Kim, J.-H., Dorhout, D., Baas, M., and Damsté, J.S.S.: Sources and distributions of branched tetraether lipids and crenarchaeol along the Portuguese continental margin: Implications for the BIT index, Cont. Shelf Res., 96, 34–44, 2015.

Zorita, E., Kharin, V., and Vonstorch, H.: The Atmospheric Circulation and Sea-Surface Temperature in the North-Atlantic Area in Winter - Their Interaction and Relevance for Iberian Precipitation, J. Climatol., 5, 1097–1108, 1992.

Biogeosciences Discuss., doi:10.5194/bg-2016-146, 2016
Manuscript under review for journal Biogeosciences
Published: 30 May 2016

945 **Table 1** provides the stations, sediment core names, locations of sampling and water depth for
946 each sediment core used in this study.

Station	Core name	Latitude [N]	Longitude [W]	Water depth [m]
0501.029	Tagus River Floodplain	39° 23' 07.80"	08° 31' 55.56"	0
64PE332-30-2	Tagus Mudbelt	38° 39' 02.20"	09° 28' 07.68"	82
64PE332-44-2	Lisbon Canyon Head	38° 30' 20.19"	09° 15' 04.87"	259
64PE269-39-4	Lower Setúbal Canyon	38° 13' 12.00"	10° 10' 00.00"	4217

947
948
949
950
951
952
953
954
955
956
957
958
959
960

Biogeosciences Discuss., doi:10.5194/bg-2016-146, 2016
Manuscript under review for journal Biogeosciences
Published: 30 May 2016

961 **Table 2** summarizes the data used to determine an age depth model for the sediment samples

962 in this study. [a]Data is from Vis et al., (2008).

Sediment core	Lab code	Depth in core [cm]	Mean depth in core [cm]	Uncorrected AMS ^{14}C ages [yr BP]	Analytical error (±1σ) [yrs]	Ages (ΔR = 0 yr) (±2σ) [cal yr BP]	Ages [cal yr BP]	Analyzed material
0501.029[a]		0-2	1				0	
0501.029[a]		331-334	332.5	1136	38	964-1150	1057	Roots of fraction>125µm
0501.029[a]		331-334	332.5	1022	37	901-1001	951	Total organic fraction>125µm
0501.029[a]		604-607	605.5	3089	38	3209-3383	3296	Terrestrial botanical macrofossils
0501.029[a]		711-712	711.5	4129	42	4530-4821	4676	Terrestrial botanical macrofossils
0501.029[a]		1024-1029	1026.5	5790	40	6485-6676	6581	Terrestrial botanical macrofossils
0501.029[a]		1046-1050	1048	5900	45	6633-6805	6719	Terrestrial botanical macrofossils
64PE332-30-2		0-2	1				0	
64PE332-30-2	BETA 348791	20-22	21	500	30	40-236	138	Gastropod fragments
64PE332-30-2	BETA 348792	428-430	429	1730	30	1221-1349	1285	*Ammonia beccarii* (benthic forams)
64PE332-30-2	BETA 348793	678-680	679	2320	30	1848-2032	1940	Gastropod
64PE332-30-2	BETA 317911	976-978	977	5370	30	5643-5849	5746	Bivalve shell fragments
64PE332-44-2		0-2	1				0	
64PE332-44-2	BETA 317906	521-523	521.5	2330	30	1858-2044	1951	Mixed planktonic forams
64PE332-44-2	BETA 317907	770-772	771.5	5390	30	5664-5865	5765	Gastropod
64PE332-44-2	BETA 317908	924.5-926.5	925.5	8160	40	8515-8798	8657	Mixed planktonic forams
64PE269-39-4		0	0				0	
64PE269-39-4	BETA 330562	5	5	930	30	486-608	547	G. bulloides (planktonic forams)
64PE269-39-4	BETA 330563	100	100	4980	50	5205-5466	5336	G. bulloides (planktonic forams)
64PE269-39-4	BETA 330564	200	200	10190	40	11092-11271	11182	G. bulloides (planktonic forams)
64PE269-39-4	BETA 348794	280	280	11540	40	12865-13150	13008	G. bulloides (planktonic forams)

Biogeosciences Discuss., doi:10.5194/bg-2016-146, 2016
Manuscript under review for journal Biogeosciences
Published: 30 May 2016

963 **Table 3.** Concentrations of GDGTs and brGDGT based indices for each sample set along the

964 transect. Values in red were previously published in Zell et al., (2014).

Sample name	Age (cal. kyrs. BP)	TOC (wt. %)	$\delta^{13}C_{TOC}$ (‰ VPDB)	Crenarchaeol (µg gOC^{-1})	Sum brGDGTs (µg gOC^{-1})	BIT index	MBT'_{5me}	DC'	IR	IR IIa	IR IIIa
Tagus soils											
TRS-8b	n/a	3.0	-27.8	2.2	19.2	0.88	0.51	0.13	0.39	0.36	0.43
TRS-7	n/a	5.0	-27.5	0.0	7.5	1.00	0.56	0.01	0.13	0.12	0.17
TRS-9	n/a	0.5	-27.2	0.1	7.8	0.99	0.68	0.01	0.14	0.14	0.15
TRS-3	n/a	0.7	-29.0	0.6	4.1	0.87	0.40	0.05	0.41	0.43	0.39
TRS-4	n/a	0.7	-28.7	1.2	5.3	0.81	0.42	0.04	0.39	0.41	0.30
TRS-5	n/a	2.2	-28.4	2.4	15.3	0.85	0.29	0.10	0.37	0.37	0.35
TRS-10	n/a	1.5	-28.5	1.4	1.6	0.49	0.60	0.19	0.84	0.88	0.83
TRS-12	n/a	0.2	-25.1	4.0	2.4	0.34	0.62	0.22	0.87	0.87	0.91
TRS-14b	n/a	0.8	-25.3	1.7	2.1	0.48	0.57	0.32	0.85	0.89	0.86
TRS-13	n/a	6.9	-27.0	0.9	1.2	0.54	0.33	0.13	0.74	0.80	0.71
TRS-15	n/a	0.9	-25.7	1.9	2.0	0.48	0.46	0.21	0.86	0.90	0.86
TRS-16	n/a	0.1	-24.8	1.6	3.0	0.62	0.56	0.19	0.92	0.93	0.93
TRS-20	n/a	0.1	-26.1	0.6	3.8	0.84	0.52	0.38	0.83	0.87	0.83
TRS-19	n/a	0.1	-25.7	0.7	19.7	0.95	0.56	0.44	0.84	0.85	0.89
Tagus Riverbank sediments											
TRS-6	n/a	1.7	-26.3	16.7	76.0	0.77	0.53	0.30	0.54	0.46	0.59
TRS-8a	n/a	0.2	-26.5	10.8	68.2	0.83	0.55	0.26	0.77	0.71	0.83
TRS 2a	n/a	3.3	-23.6	3.4	12.8	0.70	0.63	0.42	0.79	0.81	0.77
TRS 2b	n/a	0.5	-25.1	8.1	55.1	0.80	0.57	0.45	0.67	0.72	0.72
TRS 1a	n/a	0.9	-26.9	9.7	18.8	0.62	0.54	0.21	0.68	0.68	0.66
TRS1b	n/a	1.5	-27.6	26.1	19.7	0.28	0.64	0.53	0.72	0.82	0.80
TRS-11	n/a	1.3	-27.0	6.3	3.9	0.33	0.48	0.24	0.75	0.79	0.75
TRS-14a	n/a	3.0	-27.1	1.2	21.7	0.92	0.38	0.44	0.55	0.56	0.68
TRS-17	n/a	3.7	-29.6	1.6	37.8	0.93	0.41	0.51	0.70	0.65	0.66
TRS-22	n/a	0.6	-29.8	3.1	24.8	0.86	0.41	0.40	0.80	0.75	0.82
Tagus River SPM											
TR 2 Sup July	n/a	2.6	-29.2	6.2	33.1	0.80	0.51	0.28	0.60	0.53	0.64
TR 3#1 –Sup Sept.	n/a	1.8	-28.4	5.6	20.7	0.73	0.52	0.30	0.59	0.51	0.61
TR4 #1 Oct.	n/a	2.5	-30.9	8.6	38.1	0.77	0.52	0.30	0.61	0.54	0.62
TR5 #1 Sup Nov.	n/a	1.3	-28.9	5.8	54.8	0.85	0.49	0.25	0.62	0.55	0.68
TR 6 #1 Sup Dec.	n/a	2.4	-29.4	11.5	86.8	0.85	0.47	0.26	0.63	0.56	0.67
TR7 #1 Sup Jan.	n/a	2.4	-29.8	9.8	53.6	0.77	0.48	0.27	0.63	0.56	0.67
TR8 #1 Sup Feb.	n/a	1.0	-29.4	16.8	46.9	0.69	0.50	0.27	0.58	0.51	0.62
TR9 #1 Sup Mar.	n/a	2.2	-29.0	6.3	21.9	0.72	0.50	0.29	0.58	0.51	0.61
TR10 #1 Sup Apr.	n/a	1.9	-28.5	0.8	36.5	0.96	0.52	0.29	0.58	0.50	0.61
TR11 #1 Sup May	n/a	1.7	-28.5	26.3	80.8	0.69	0.52	0.29	0.56	0.48	0.59
TR12 #1 Sup June	n/a	1.3	-27.8	9.5	22.8	0.65	0.55	0.23	0.51	0.48	0.58
Tagus River Floodplain											

Biogeosciences Discuss., doi:10.5194/bg-2016-146, 2016
Manuscript under review for journal Biogeosciences
Published: 30 May 2016

sediments (0501.029) depth (cm)											
10.0	0.0	1.7	-26.3	2.1	29.7	0.92	0.34	0.31	0.39	0.39	0.44
95.0	0.3	2.6	-26.5	6.4	66.8	0.89	0.36	0.24	0.43	0.43	0.45
195.0	0.6	1.5	-27.4	2.5	111.8	0.97	0.34	0.37	0.38	0.40	0.43
241.0	0.8	1.5	-26.0	5.2	62.0	0.90	0.40	0.24	0.35	0.36	0.38
341.5	1.0	11.2	-27.5	0.9	47.6	0.97	0.45	0.39	0.36	0.34	0.37
401.0	1.5	12.1	-27.7	1.2	90.6	0.98	0.38	0.38	0.40	0.36	0.46
453.0	2.0	8.0	-26.7	3.0	120.9	0.97	0.34	0.35	0.43	0.43	0.50
542.0	2.8	7.7	-27.3	3.2	91.9	0.95	0.37	0.39	0.40	0.41	0.42
577.0	3.1	4.6	-27.2	3.3	84.2	0.95	0.43	0.35	0.38	0.37	0.41
641.0	3.8	5.3	-28.1	1.0	59.6	0.97	0.52	0.39	0.34	0.35	0.39
681.0	4.3	6.6	-28.6	1.0	52.3	0.97	0.46	0.45	0.37	0.37	0.42
741.0	4.9	4.2	-24.4	4.2	74.3	0.92	0.43	0.45	0.38	0.38	0.36
862.0	5.6	16.2	-26.8	2.2	58.4	0.94	0.45	0.45	0.46	0.43	0.52
982.0	6.3	8.7	-27.7	1.5	46.5	0.95	0.46	0.49	0.37	0.36	0.37
1041.0	6.7	5.2	-27.2	4.4	48.2	0.87	0.48	0.45	0.40	0.39	0.41
Mudbelt sediments (64PE332-30-2) depth (cm)											
1.0	0.0	1.2	-23.7	200.9	28.5	0.09	0.58	0.35	0.51	0.45	0.54
25.0	0.2	1.0	-24.2	194.7	40.7	0.13	0.54	0.28	0.49	0.43	0.52
53.0	0.2	0.9	-24.5	189.3	36.4	0.13	0.52	0.26	0.47	0.44	0.50
75.0	0.3	1.0	-24.4	206.5	43.8	0.14	0.52	0.26	0.48	0.43	0.51
101.0	0.4	0.9	-24.3	228.9	44.4	0.13	0.53	0.27	0.48	0.43	0.51
151.0	0.5	0.9	-24.3	194.8	40.2	0.13	0.53	0.27	0.49	0.44	0.53
201.0	0.6	1.0	-24.5	187.9	31.9	0.11	0.51	0.27	0.47	0.43	0.50
248.0	0.8	0.6	-24.5	224.0	58.0	0.14	0.53	0.26	0.46	0.42	0.49
297.0	0.9	1.1	-24.5	168.3	30.6	0.12	0.50	0.26	0.47	0.42	0.51
347.0	1.1	1.0	-24.1	202.5	24.3	0.08	0.52	0.30	0.50	0.45	0.53
397.0	1.2	1.1	-24.1	180.4	27.3	0.10	0.49	0.30	0.48	0.43	0.52
429.0	1.3	1.2	-24.0	77.3	8.7	0.08	0.50	0.34	0.53	0.45	0.57
496.0	1.5	1.0	-24.3	143.8	15.1	0.07	0.52	0.32	0.53	0.46	0.57
546.0	1.6	0.9	-24.1	11.2	1.4	0.08	0.52	0.33	0.51	0.45	0.55
596.0	1.7	1.1	-27.3	141.3	14.8	0.07	0.51	0.34	0.52	0.45	0.56
645.0	1.9	1.1	-29.9	108.7	12.8	0.08	0.52	0.34	0.52	0.45	0.55
680.0	2.0	1.1	-27.4	142.1	17.4	0.08	0.54	0.31	0.50	0.44	0.54
741.0	2.7	0.8	-27.3	176.1	16.0	0.06	0.52	0.35	0.53	0.46	0.55
791.0	3.4	0.7	-24.5	240.8	19.8	0.05	0.50	0.37	0.55	0.48	0.58
840.0	4.0	0.9	-24.4	139.3	11.0	0.05	0.48	0.37	0.54	0.48	0.55
890.0	4.6	0.6	-24.6	180.2	14.2	0.05	0.48	0.39	0.55	0.47	0.57
977.0	5.7	0.7	-27.5	125.8	11.8	0.06	0.46	0.40	0.53	0.46	0.52
Lisbon Canyon Head sediments (64PE332-44-2) depth (cm)											
1.0	0.0	1.5	22.9	420.5	27.1	0.04	0.60	0.41	0.55	0.48	0.56
45.0	0.2	1.2	-22.8	409.9	47.3	0.07	0.58	0.40	0.55	0.48	0.57
85.0	0.3	1.1	-23.4	440.4	48.1	0.07	0.54	0.36	0.53	0.46	0.55

Biogeosciences Discuss., doi:10.5194/bg-2016-146, 2016
Manuscript under review for journal Biogeosciences
Published: 30 May 2016

130.5	0.5	1.2	-23.4	429.6	41.2	0.06	0.55	0.36	0.53	0.46	0.57
187.5	0.7	1.2	-23.7	308.4	27.6	0.06	0.56	0.36	0.53	0.45	0.56
221.5	0.8	1.1	-24.4	157.9	35.1	0.12	0.54	0.28	0.47	0.42	0.51
278.5	1.0	1.2	-23.2	283.6	22.7	0.05	0.54	0.36	0.51	0.45	0.54
326.5	1.2	1.0	-22.6	361.7	31.1	0.05	0.53	0.42	0.56	0.47	0.60
371.5	1.4	1.1	-22.6	374.1	26.5	0.05	0.53	0.41	0.55	0.47	0.58
429.0	1.6	1.0	-22.6	399.6	29.2	0.05	0.55	0.42	0.56	0.49	0.59
480.0	1.8	1.1	-23.4	242.3	18.0	0.05	0.54	0.41	0.55	0.48	0.57
502.0	1.9	1.1	-23.9	365.1	25.4	0.04	0.52	0.42	0.56	0.49	0.58
522.0	2.0	1.0	-23.4	376.8	30.9	0.05	0.55	0.39	0.55	0.48	0.57
550.0	2.4	1.0	-23.0	363.1	26.7	0.05	0.54	0.43	0.57	0.50	0.59
570.0	2.7	0.7	-22.6	493.6	34.3	0.04	0.53	0.43	0.57	0.50	0.59
630.0	3.6	0.7	-22.4	389.6	25.7	0.04	0.53	0.44	0.58	0.51	0.60
686.0	4.5	0.5	-22.4	640.2	40.7	0.04	0.54	0.45	0.59	0.51	0.60
728.0	5.1	0.5	-22.1	100.1	6.7	0.04	0.50	0.45	0.57	0.51	0.58
771.0	5.8	0.7	-23.3	620.7	37.3	0.04	0.53	0.44	0.58	0.50	0.59
805.0	6.4	0.3	-22.1	414.0	25.9	0.04	0.52	0.45	0.58	0.51	0.58
869.5	7.6	0.3	-22.3	538.9	35.7	0.04	0.54	0.41	0.57	0.50	0.56
925.5	8.7	0.3	-23.1	409.4	30.1	0.04	0.52	0.46	0.59	0.51	0.58
Lower Setúbal Canyon sediments (64PE269-39-4) depth (cm)											
1.0	0.0	0.8	-23.5	265.3	20.3	0.05	0.68	0.38	0.73	0.60	0.77
20.0	1.3	0.7	-22.3	506.5	15.6	0.02	0.60	0.39	0.77	0.60	0.80
40.0	2.3	0.6	-22.0	751.5	18.1	0.02	0.58	0.39	0.73	0.61	0.75
60.0	3.3	0.8	-22.2	540.7	16.2	0.02	0.56	0.46	0.75	0.61	0.74
80.0	4.3	0.8	-22.3	460.5	13.5	0.02	0.56	0.41	0.75	0.63	0.77
100.0	5.3	0.8	-22.8	204.7	7.3	0.03	0.57	0.37	0.74	0.66	0.75
120.0	6.5	0.7	-22.8	199.2	8.0	0.03	0.57	0.38	0.77	0.66	0.78
140.0	7.7	0.5	-26.1	433.3	13.6	0.02	0.51	0.41	0.73	0.67	0.74
160.0	8.8	0.5	-22.8	395.6	16.9	0.03	0.45	0.43	0.69	0.64	0.64
180.0	10.0	0.4	-24.9	709.2	25.6	0.02	0.48	0.43	0.69	0.58	0.65
200.0	11.2	0.5	-25.7	703.9	22.1	0.02	0.54	0.41	0.66	0.52	0.64
220.0	11.6	n/a	n/a	n/a	n/a	0.02	0.48	0.47	0.66	0.52	0.59
240.0	12.1	n/a	n/a	n/a	n/a	0.01	0.56	0.57	0.70	0.56	0.63
260.0	12.6	n/a	n/a	n/a	n/a	0.03	0.58	0.49	0.71	0.58	0.64
280.0	13.0	n/a	n/a	n/a	n/a	0.01	0.52	0.48	0.69	0.57	0.65

965

966

967

Biogeosciences Discuss., doi:10.5194/bg-2016-146, 2016
Manuscript under review for journal Biogeosciences
Published: 30 May 2016

Biogeosciences Discussions
Open Access
EGU

Figure 1

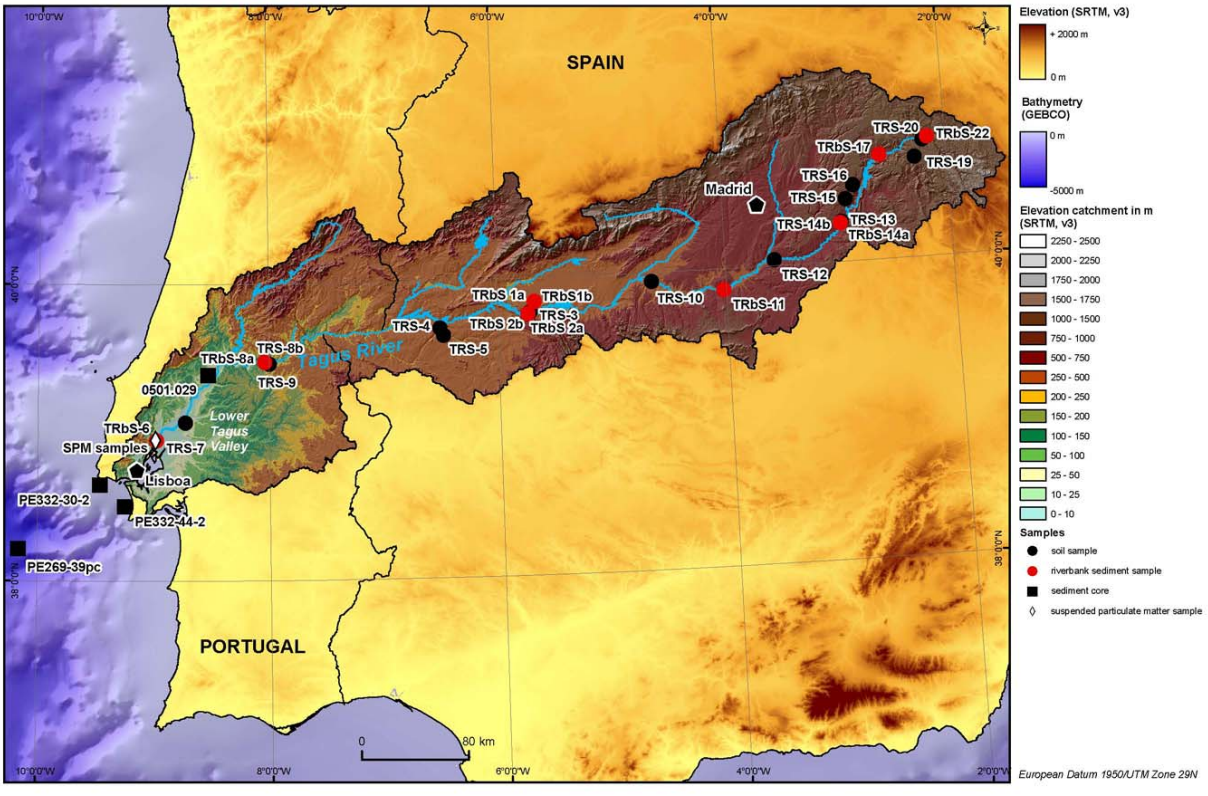

Biogeosciences Discuss., doi:10.5194/bg-2016-146, 2016
Manuscript under review for journal Biogeosciences
Published: 30 May 2016

Figure 2

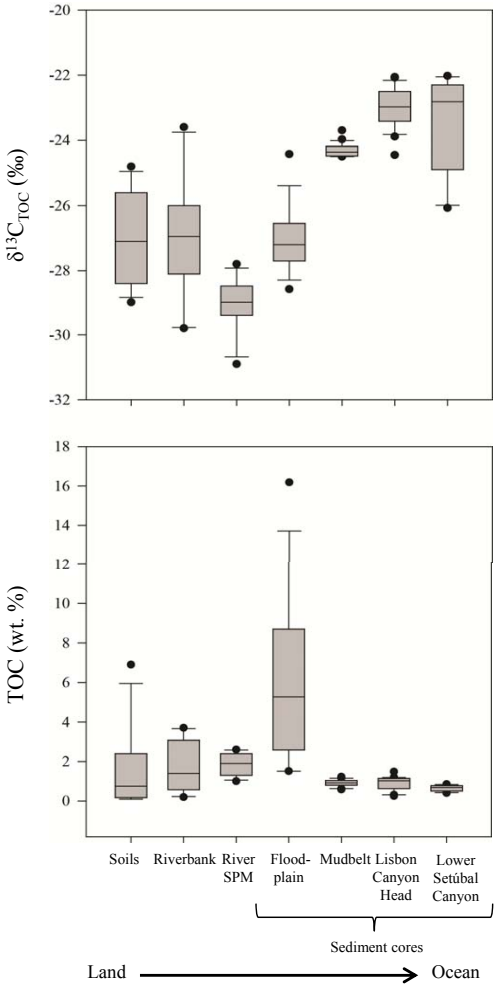

Biogeosciences Discuss., doi:10.5194/bg-2016-146, 2016
Manuscript under review for journal Biogeosciences
Published: 30 May 2016

Figure 3

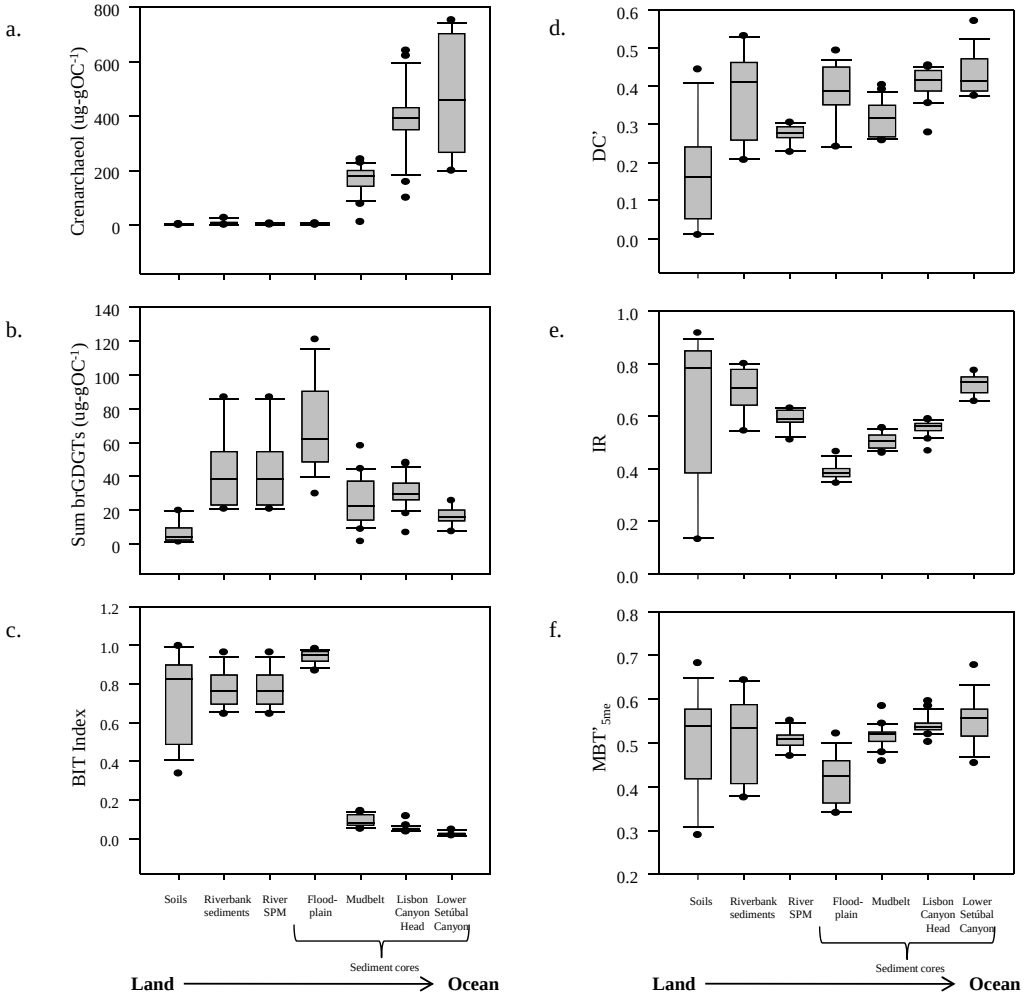

Biogeosciences Discuss., doi:10.5194/bg-2016-146, 2016
Manuscript under review for journal Biogeosciences
Published: 30 May 2016

Figure 4

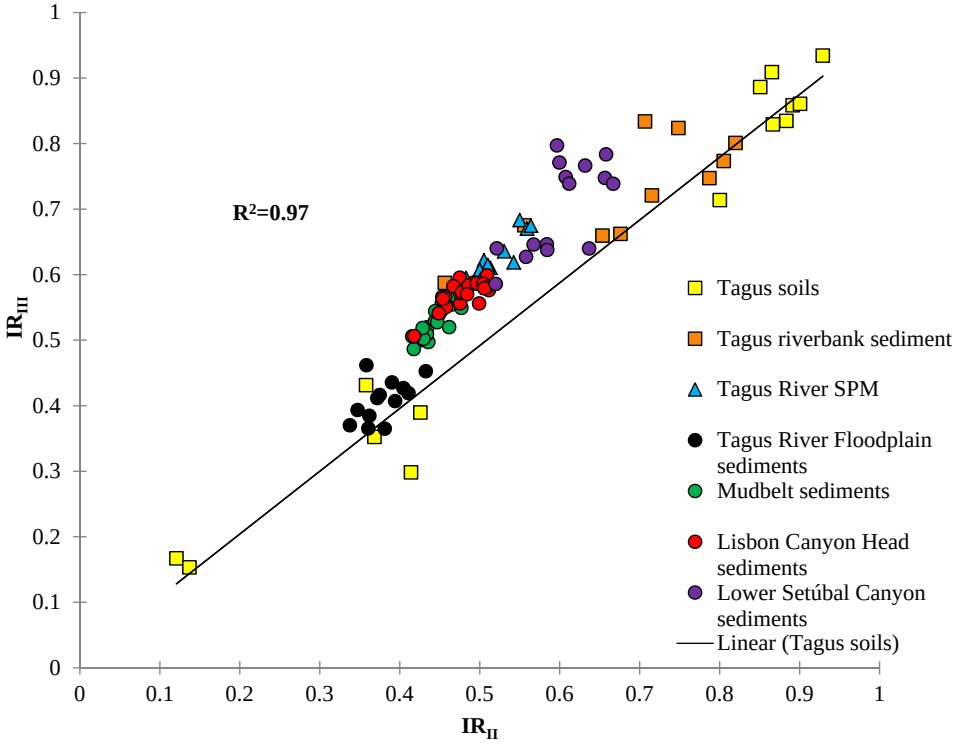

Biogeosciences Discuss., doi:10.5194/bg-2016-146, 2016
Manuscript under review for journal Biogeosciences
Published: 30 May 2016

Figure 5

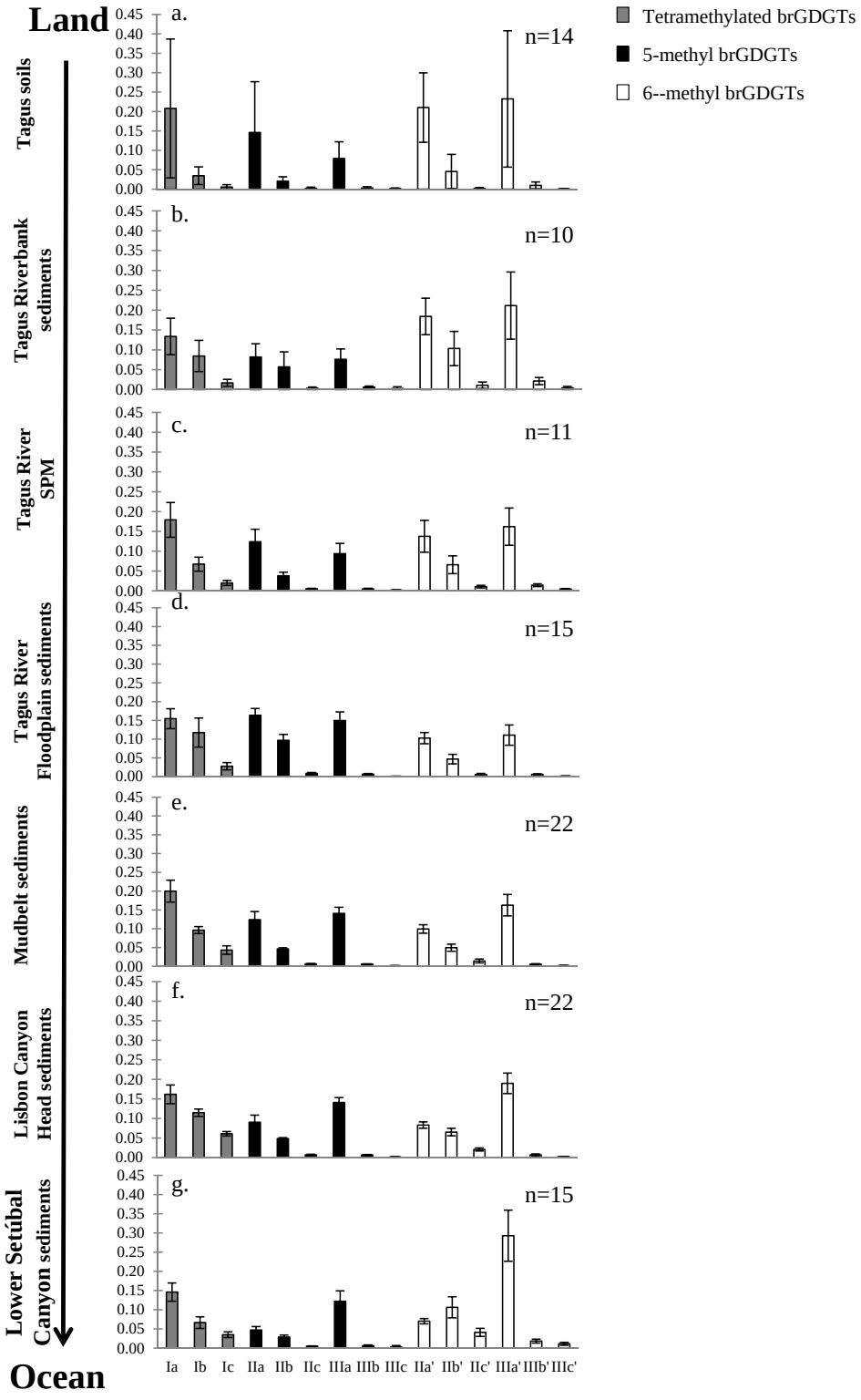

Biogeosciences Discuss., doi:10.5194/bg-2016-146, 2016
Manuscript under review for journal Biogeosciences
Published: 30 May 2016

Figure 6

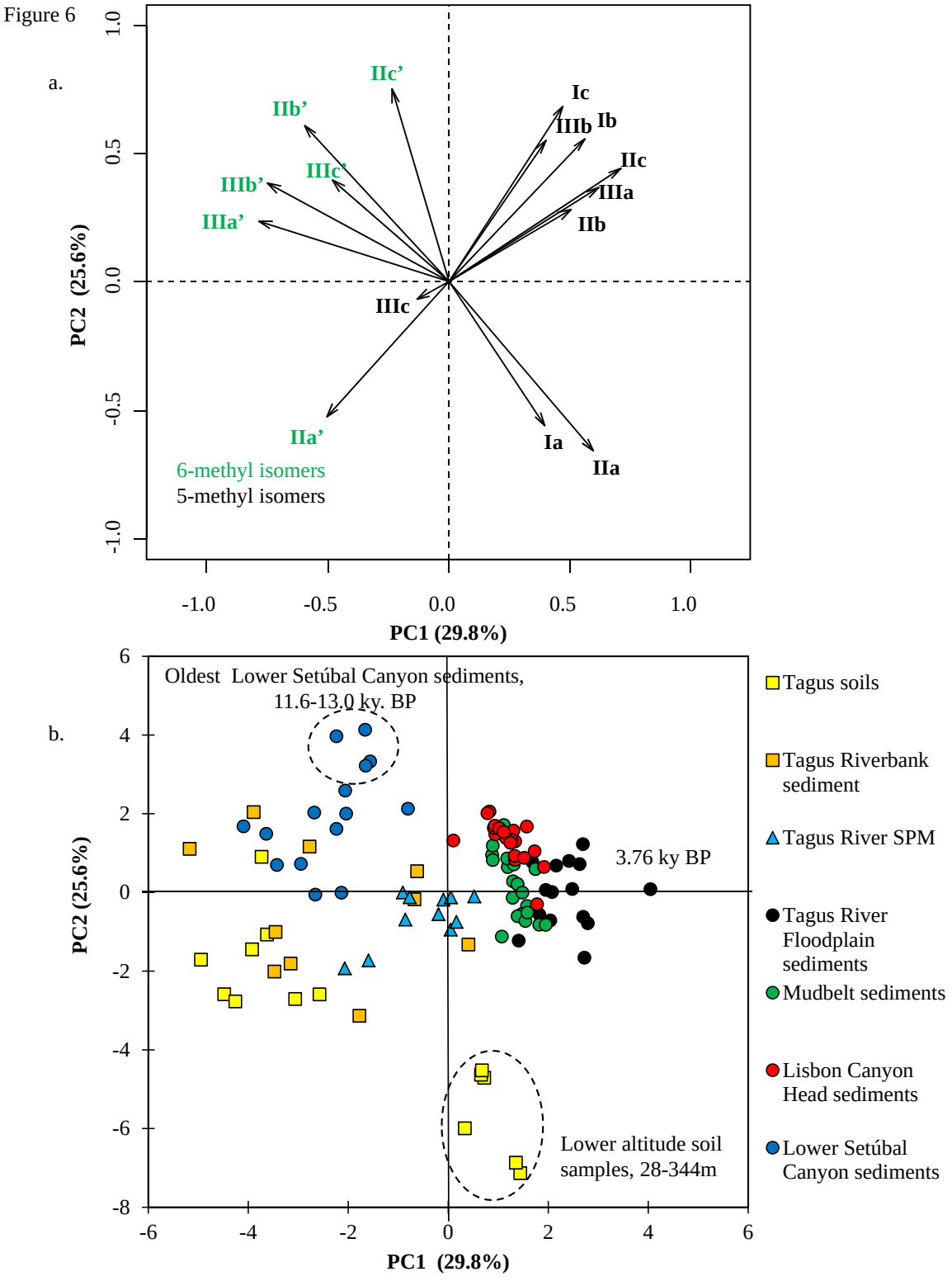

Biogeosciences Discuss., doi:10.5194/bg-2016-146, 2016
Manuscript under review for journal Biogeosciences
Published: 30 May 2016

Fig. 7

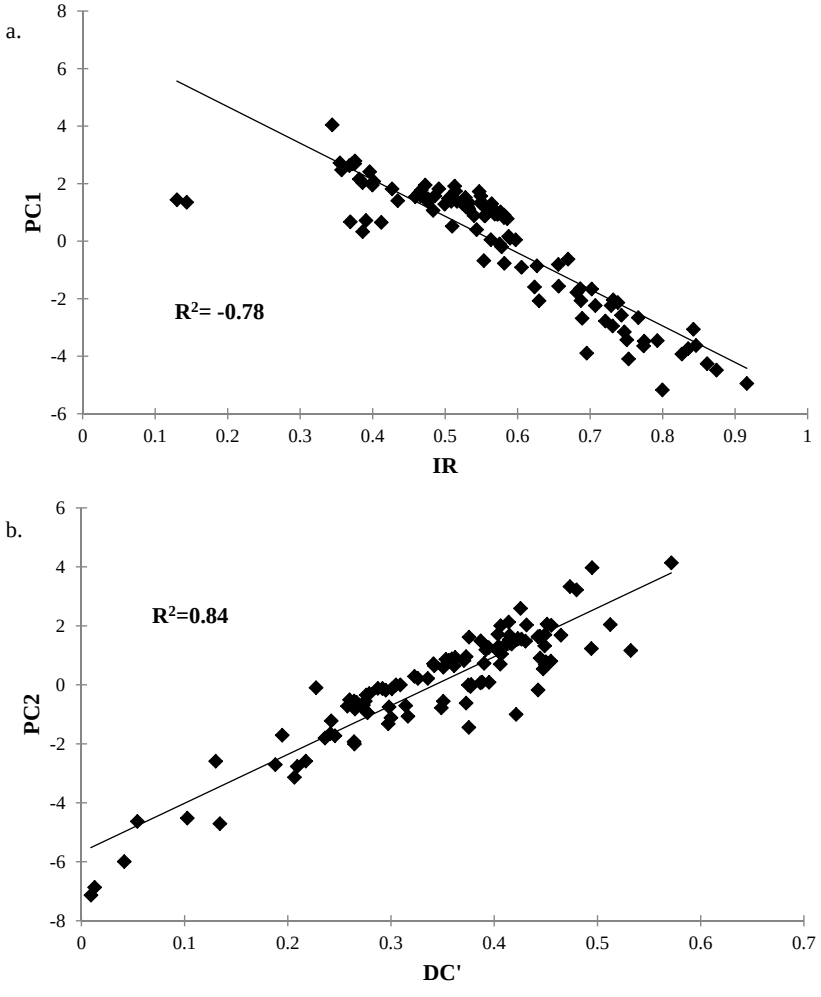

Biogeosciences Discuss., doi:10.5194/bg-2016-146, 2016
Manuscript under review for journal Biogeosciences
Published: 30 May 2016

Figure 8

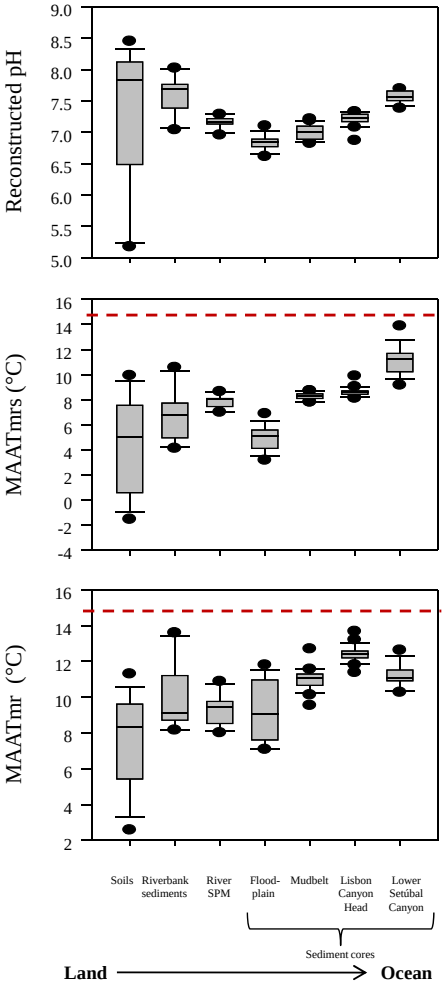

Biogeosciences Discuss., doi:10.5194/bg-2016-146, 2016
Manuscript under review for journal Biogeosciences
Published: 30 May 2016

Biogeosciences Discussions
Open Access
EGU

Figure 9

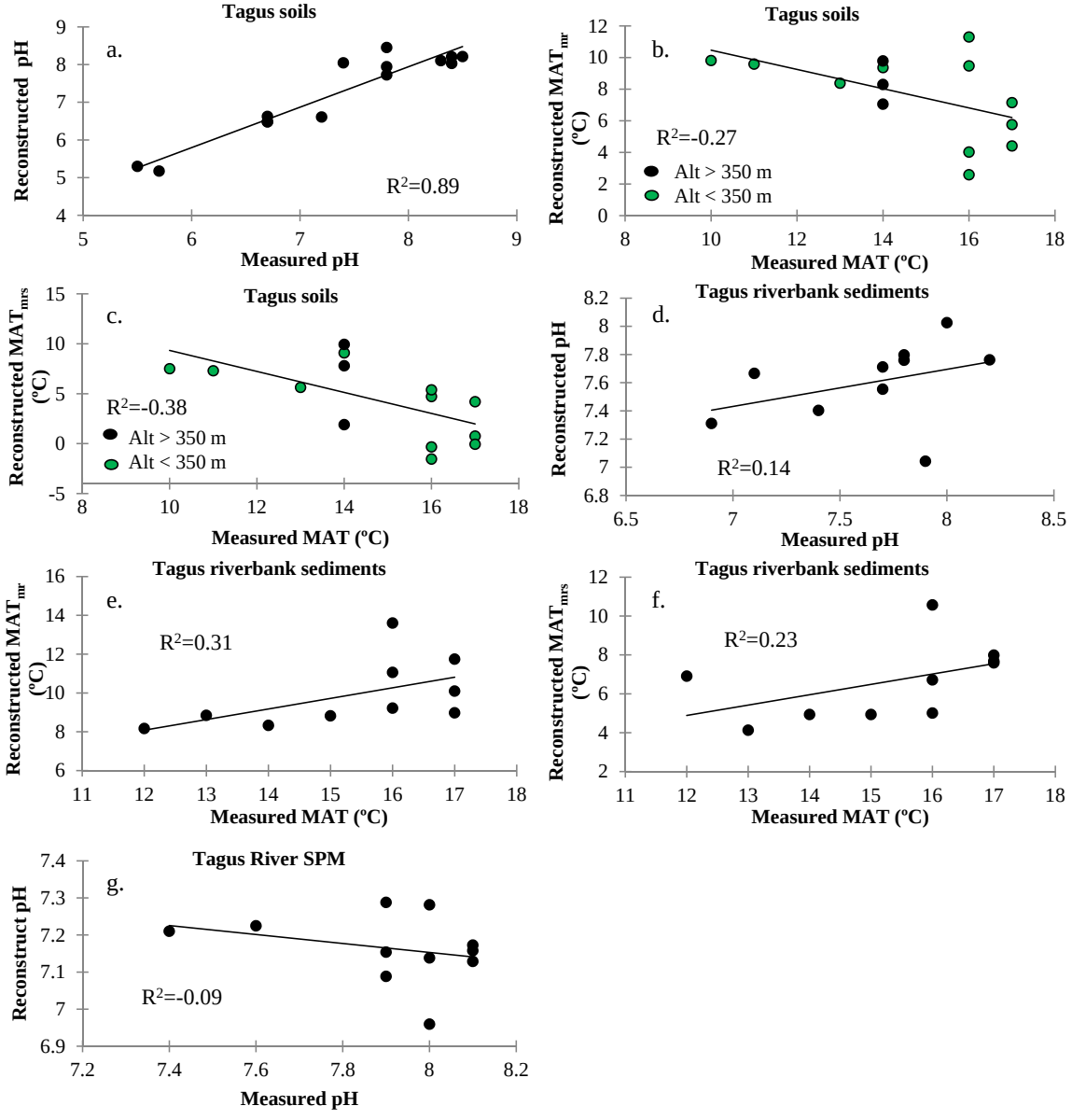

Biogeosciences Discuss., doi:10.5194/bg-2016-146, 2016
Manuscript under review for journal Biogeosciences
Published: 30 May 2016

Figure 10